CISPLATIN RESISTANCE AND ERBB3 IN BLADDER CANCER

A Thesis

Presented to the faculty of the Department of Biological Sciences

California State University, Sacramento

Submitted in partial satisfaction of
the requirements for the degree of

MASTER OF SCIENCE

in

Biological Sciences

(Molecular and Cellular Biology)

by

Benjamin Asher Mooso

FALL
2014

CISPLATIN RESISTANCE AND ERBB3 IN BLADDER CANCER

A Thesis

by

Benjamin Mooso

Approved by:

_____, Committee Chair
Dr. Susanne Lindgren

_____, Second Reader
Dr. Paramita Ghosh

_____, Third Reader
Dr. Hao Nguyen

_____
Date

Student: Benjamin Mooso

I certify that this student has met the requirements for format contained in the University format manual, and that this thesis is suitable for shelving in the Library and credit is to be awarded for the thesis.

_____, Graduate Coordinator _____
Dr. Jamie Kneitel Date

Department of Biological Sciences

Abstract

of

CISPLATIN RESISTANCE AND ERBB3 IN BLADDER CANCER

by

Benjamin Mooso

Bladder cancer is among the leading causes of cancer in the Western and developing world. Left undetected and untreated, this disease progresses from its initial stages into muscle-invasive bladder cancer (MIBC) which is significantly more aggressive and difficult to treat. Current treatment for MIBC is platinum-based chemotherapy, which is highly toxic to the patient. This chemotherapeutic regimen utilizes cisplatin in combination with two to four other chemotherapeutics. In addition to being highly toxic, this regimen is sometimes ineffective due to intrinsic or acquired cisplatin resistance. Due to this, new therapeutic targets have been sought.

One likely candidate is the ErbB family of receptor tyrosine kinases, which have been shown to be upregulated in MIBC. Due to their role in cell survival, and their utility as therapeutic targets in other epithelial cancers, many clinical trials have been conducted to assess the utility of ErbB inhibitors in the treatment of MIBC. Unfortunately, none of these studies has shown any added benefit over standard platinum-based chemotherapy. This study was undertaken to elucidate the mechanisms by which the ErbB family and cisplatin interact within the bladder cancer cell.

Four established bladder cancer cell lines, T24, TCCSUP, J82, and RT4, were used for this study to provide a broader representation of MIBC. The T24 and TCCSUP cell lines were derived from women, while the J82 and RT4 cell lines were derived from men. Cells were treated with various ErbB inhibitors as well as cisplatin. Cells were also transfected with siRNA against EGFR, ErbB2, and ErbB3 to knockdown expression of these ErbB family members in these cells. Cells were analyzed for growth via MTT assay, as well as apoptosis and cell cycle distribution by flow cytometry. Cell lysates were further probed by Western Blot for protein expression levels and protein activation.

Western Blot results revealed that the cell lines chosen had ErbB family expression consistent with the literature, except the RT4 cell line which expressed very low levels of all four ErbB family members. MTT assay demonstrated that the T24, TCCSUP, and RT4 cell lines were all resistant to cisplatin treatment, while the J82 cell line was sensitive to cisplatin. MTT assay further showed that knockdown of EGFR via siRNA was more effective at inhibiting cellular growth than ErbB2 knockdown. While flow cytometry revealed that neither siRNA had a major effect on apoptosis in any cell line, it also revealed that cisplatin induced a growth arrest in the J82 cell line by causing a G2 arrest of the cell cycle. While ErbB3 siRNA was ineffective at knocking down ErbB3 expression in all cell lines except J82, this was determined to be caused by an increase in ErbB3 protein stability in these cell lines. In the J82 cell line, ErbB3 knockdown significantly inhibited cellular growth, and trended towards an increase in apoptosis.

Probing of cellular lysates revealed that no common pattern of ErbB family phosphorylation sites was activated between the four cell lines. However, cisplatin-resistant cell lines did trend toward an increase in activation of the downstream effector ERK upon treatment with cisplatin. However, ERK phosphorylation was not able to be reliably inhibited by ErbB inhibitors during ligand-induced activation. While growth assays demonstrated the ability of various combinations of ErbB inhibitors to retard cellular growth, no one drug combination was determined to be the best. In addition, no drug combination tested was observed to have a significant effect on apoptosis or cell cycle distribution of bladder cancer cell lines.

The current study points to the importance of the ErbB family in the broad cancer treatment landscape, and demonstrates the desperate need for new therapies which target this family by unconventional methods. Taking advantage of this information, in combination with current treatment regimens and cancer knowledge, will help the medical community to better serve the population of MIBC patients.

_____, Committee Chair
Dr. Susanne Lindgren

_____
Date

ACKNOWLEDGEMENTS

I would like to thank Dr. Paramita Ghosh for all of her support, for providing the idea for this thesis, for giving me advice when I most needed it, and allowing me to work in her laboratory while completing this work. She was the first to introduce me to the practical world of scientific inquiry in a real-real world setting. Dr. Ghosh took a huge chance in bringing me into her laboratory and I am truly grateful for all of the opportunities she has afforded me.

I would also like to thank Dr. Susanne Lindgren for serving as my on-campus advisor and for allowing me to do my thesis work in Dr. Ghosh's laboratory. As graduate coordinator Dr. Lindgren took a huge chance on me by taking me on as a graduate student under her advisement when my prior academic achievements would not have merited such action. In addition, her invaluable knowledge of the Sac State system provided me with a wonderful resource to navigate my way through my coursework and thesis.

I would like to thank the UC Davis Medical Center Comprehensive Cancer Center for providing the funding for this study and for providing the trastuzumab used in this study. I would also like to thank Dr. Ralph deVere White and Dr. Chong-Xian Pan for providing me with technical assistance in this study. I would like to thank the VA Northern California Health Care System (VANCHCS) in Sacramento, CA for

providing lab space and equipment used in this study. The contents reported/presented within do not represent the views of the Department of Veterans Affairs or the United States Government. Additionally, I would like to thank the leadership of the Research Service at VANCHCS for allowing me to conduct my thesis research and providing for me to present my results at the American Association of Cancer Researchers (AACR) Annual Conference in 2014. Specifically I would like to thank Dr. Barth Wilsey, Dr. David Asmuth, Dr. Robert O'Donnell, Jefferson Lee, Jeanette Rainey, Stephanie Brown, and Laura Jones.

I would like to thank all of the members of the Ghosh Lab, past and present, who have helped me to develop and hone the techniques I have today, especially Duanna Challenger, Dr. Salma Siddiqui, Thomas Steele, Ryan Beggs, Anisha Madhav, Dr. Liqun Chen, Dr. Swagata Bose, Rosalinda Savoy, Maitreyee Jathal, Leandro D'Abronzo, Jean Cheung, Sherra Johnson, and Elyse van Spyk.

I would like to thank Dr. Maria Mudryj and Dr. Ruth Vinall for providing me with advice both on my thesis and navigating the scientific world. Similarly, I would like to thank Dr. Hao Nguyen for agreeing to be a part of my supervisory committee and providing invaluable advice and feedback.

Lastly, I would like to thank my partner, Jim, for all of his support during these long three years. His patience while I spent long evenings and weekends in the lab allowed me to complete the necessary work to collect and compile the data necessary for this thesis. I would also like to thank my family and friends for their endless support, even when that meant sacrificing time with them.

TABLE OF CONTENTS

LIST OF TABLES

Tables Page

LIST OF FIGURES

Figures Page

INTRODUCTION

Bladder cancer is a major concern in both Western and developing countries. It is the fourth most commonly diagnosed cancer amongst men and the ninth amongst women in the United States (American Cancer Society, 2013). In the Western world, smoking and occupational exposure to toxic chemicals are the predominant risk factors for bladder cancer (Vishnu, Mathew et al. 2011). Ninety percent of newly diagnosed bladder cancers arise from the transitional epithelium, an epithelial layer of cells that lines the urinary tract including the ureters, bladder, and urethra (Lazzeri 2006). This layer is commonly known as the urothelium and the tumors which arise from it are classified as transitional cell carcinomas (TCC) (Vishnu, Mathew et al. 2011). Six to eight percent of newly diagnosed cases of bladder cancer are squamous cell carcinomas, arising from the squamous cells of the bladder's epithelium. The remaining two percent of bladder cancer cases consist of adenocarcinomas (Vishnu, Mathew et al. 2011), tumors which arise from the urachus. The urachus is a remnant of the structure within the fetus that connects the bladder to the umbilical cord (Larsen 2001). One third of TCC cases are composed of muscle invasive bladder carcinomas (MIBC). These are tumors which have grown through the transitional epithelium and penetrated the muscle surrounding the bladder. The remaining two-thirds of TCC cases are superficial, non-muscle invasive bladder carcinomas (NMIBC) (Amsellem-Ouazana, Bièche et al. 2006). These are comprised of tumors which have not yet grown into the bladder's muscle.

Standard of care in the U.S. for a NMIBC consists of surgical removal of the tumor via transurethral resection of the tumor, followed by immunotherapy with Bacillus Calmette-Guérin (BCG). BCG is a highly immunogenic tuberculosis vaccine that is frequently used as an adjuvant due to its ability to induce a strong cellular immune response. BCG is used in post-operative NMIBC patients in order to induce a localized immune response in the bladder tissue at the margin of the surgical excision (Brincks, Risk et al. 2013). Unfortunately, in approximately 25% of all NMIBC cases treated in this manner, and 15-30% of high-grade, more advanced NMIBC cases, the cancer continues to progress. At this point the cancer develops either into a MIBC or even further into a metastatic disease (Vishnu, Mathew et al. 2011). MIBC strains of TCC are more aggressive and correlate with a high rate of metastasis and mortality. Metastases are commonly located in the lymph nodes, liver, lung, bone, adrenal gland and intestine (Vishnu, Mathew et al. 2011). Owing to the aggressive nature of MIBC, the current standard of care treatment for patients with MIBC is radical cystectomy (Vishnu, Mathew et al. 2011). During this procedure, the entire bladder is removed to prevent disease recurrence, and an artificial bladder is implanted. Many physicians also prescribe neoadjuvant, pre-surgical, platinum-based chemotherapy to all MIBC patients undergoing radical cystectomy (Apolo, Bochner et al. 2012). Patient prognosis following surgery is dependent upon the extent of invasion, including whether lymph node invasion is present (Zachos, Konstantinopoulos et al. 2010).

Platinum-based chemotherapy is a staple in the treatment of metastatic MIBC. One of the most common platinum-based treatments is a cocktail of methotrexate, vinblastine, doxorubicin, and cisplatin, a combination chemotherapy commonly known as MVAC. This combination is effective because it combines four mitotic inhibitors which act by starving cells of folic acid, promoting microtubule detachment, intercalating within DNA base-pairs, and crosslinking DNA, respectively. Another common regimen, abbreviated GC, combines gemcitabine and cisplatin. This regimen is less toxic than MVAC as it contains only two drugs, yet is still effective as it combines a nucleoside analog with a DNA cross-linker. Both regimens have demonstrated a response rate of approximately 45% in patients with recurrent MIBC, with a median overall survival of 14 months (Guancial, Rosenberg et al. 2011, Vishnu, Mathew et al. 2011). It is important to note that overall survival does not distinguish between causes of death and includes all people with a specific disease. In contrast, the response rate describes what percent of patients will respond to a course of treatment. The combination of these two metrics, overall survival and response rate, therefore gives a good sense of the efficacy of a specific course of treatment and are frequently used together. Even though cisplatin is one of the main chemotherapeutics in the treatment of MIBC, as noted by the fact that is present in both MVAC and GC cocktails, several clinical research scientists have suggested that cisplatin resistance is a frequent complication that ultimately limits treatment options and life expectancy (Sternberg, Yagoda et al. 1989, Wood, Anderson et al. 1992).

It has been theorized that the resistance of MIBC to platinum-based chemotherapies could be overcome by using a more personalized approach. This would involve studying the specific characteristics of individual bladder cancers, and would allow researchers to determine the mechanism of resistance. Furthermore, such a study would allow for the development and testing of therapeutics, which might re-sensitize the cancerous cells to platinum-based chemotherapies.

In an effort to find a "drugable" target for recurrent MIBC, researchers have looked at the variations in protein expression between the cancerous tissue and normal urothelium. Various studies have pointed to an increase in the expression of the epidermal growth factor receptor (EGFR) family of receptor tyrosine kinases (RTKs), in numerous solid tumors including TCC. The EGFR family, like all RTKs, are a cell surface protein molecule, which characteristically contains an extracellular receptor domain and an intracellular kinase domain (Hubbard and Till 2000). The extracellular receptor domain binds to its ligand, which results in a conformational change in the intracellular kinase domain. This then allows the protein to dimerize with another EGFR family member, and allows the kinase domain to bind ATP. ATP binding leads to phosphorylation and the initiation of signal transduction pathways within the targeted cell. The EGFR family of RTKs are phosphorylated at specific amino acid residues each corresponding to specific signaling pathways (Figure 1) (Yarden and Sliwkowski 2001). The EGFR family is made up of four structurally related molecules, each with numerous names as they were simultaneously discovered by different research

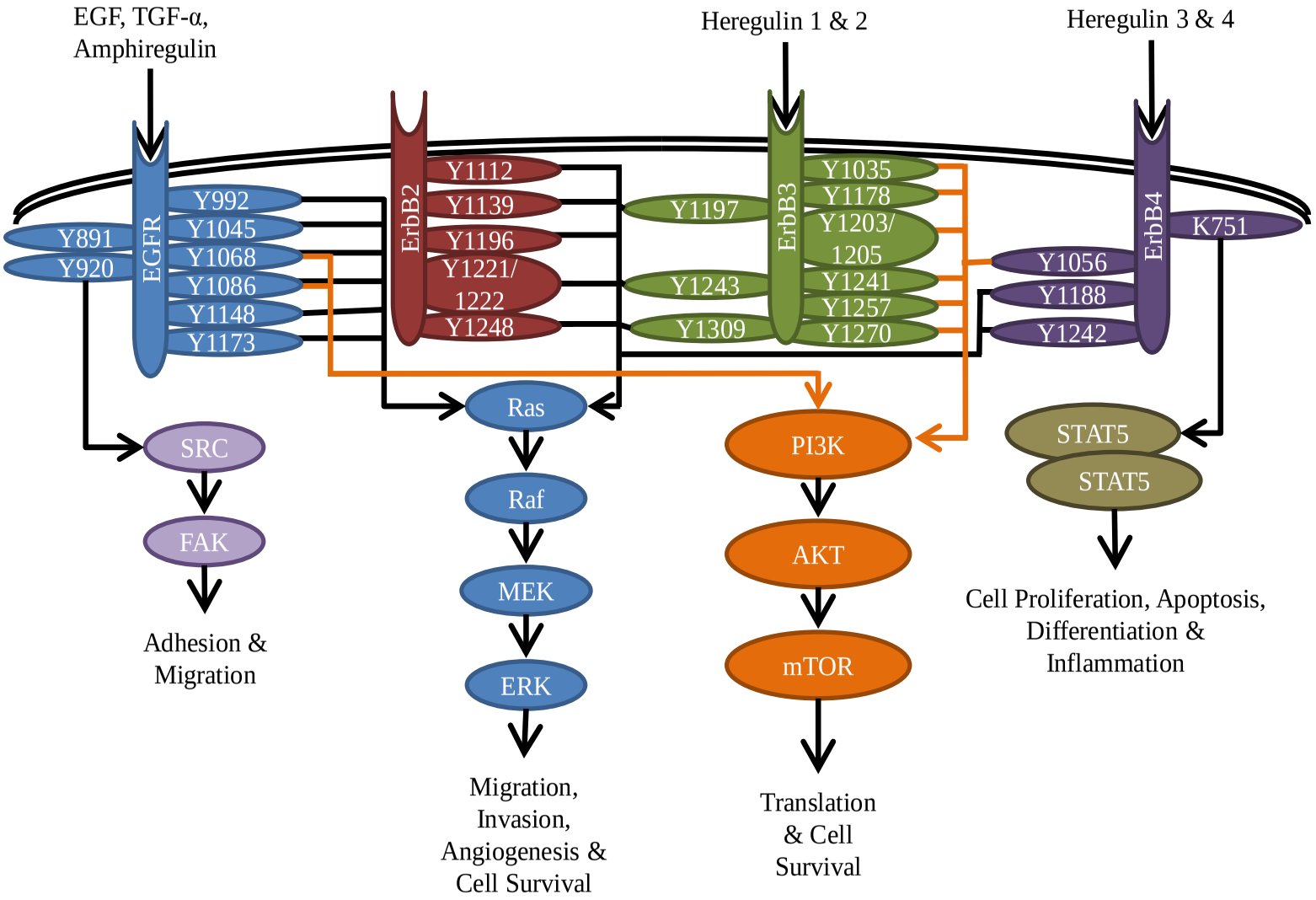

Figure 1. Graphic representation of the EGFR family phosphorylation sites and downstream effectors.

scientists, including human EGFR (ErbB1/Her1), human EGFR 2 (ErbB2/Her2/neu), human EGFR 3 (ErbB3/Her3) and human EGFR 4 (ErbB4/Her4) (Neal, Sharples et al. 1990, Chow, Liu et al. 1997, Chow, Chan et al. 2001, Chaux, Cohen et al. 2012, Mooso, Vinall et al. 2014).

In TCC, overexpression of EGFR and its family members ErbB2 and ErbB3 was observed in 36%, 9%, and 30% of cases respectively (Rajkumar, Stamp et al. 1996). This is significant as enhanced expression of these proteins can lead to both cellular dedifferentiation as well as increased proliferation (Bindels, van der Kwast et al. 2002, Sergina, Rausch et al. 2007, Messing, Gee et al. 2012). EGFR overexpression has also been correlated with invasion of cancerous cells into the muscular layer surrounding the bladder (Chow, Liu et al. 1997). Similarly, co-expression of EGFR with ErbB3 or ErbB3 with ErbB4 was more often detected in high-grade tumors, and correlated with the extent of tumor invasion (Chow, Liu et al. 1997).

Comparison with the normal urothelium showed that EGFR was expressed in the basal cells of the normal urothelium, the most immature cells of the normal urothelium, but was expressed in the superficial layer of the cancerous urothelium (Chow, Liu et al. 1997). Meanwhile ErbB2, ErbB3, and ErbB4 were present mainly in the superficial layer of the normal urothelium, the most mature and differentiated cells of the normal urothelium (Chow, Liu et al. 1997). However, a more recent study demonstrated that ErbB4 expression levels are statistically decreased in advanced bladder cancer when compared to normal urothelium (Rotterud, Nesland et al. 2005).

ErbB4 expression has been previously shown to cause cellular differentiation (Olayioye, Neve et al. 2000). Taken together, it would be expected then that all MIBC tissues would exhibit a less differentiated phenotype, and would have a propensity to grow without regard to their local environment.

Because of the high frequency of EGFR overexpression in TCC, a number of phase I and phase II chemotherapeutic trials have been conducted in patients with MIBC using EGFR and ErbB2 inhibitors (Zachos, Konstantinopoulos et al. 2010, Guancial, Rosenberg et al. 2011, Mooso, Vinall et al. 2014). Phase I trials primarily assess safety and tolerability of the drug in patients, while phase II trials assess dosing and efficacy against tumorigenesis. Several small molecule EGFR inhibitors have been tested in Phase II clinical trials in patients with MIBC including erlotinib (trade name Tarceva), and gefitinib. Both of these compounds bind the intracellular ATP binding pocket of the EGFR kinase domain and prevent EGFR activation. The monoclonal antibody trastuzumab (trade name Herceptin) prevents ErbB2 dimerization, an action which is required for activation and subsequent cellular signaling by this molecule. Trastuzumab has also been tested Phase II clinical trials against MIBC, but with less impressive results (Zachos, Konstantinopoulos et al. 2010). In response to the results of the Phase II clinical trials conducted with the previously mentioned drugs, the dual EGFR/ErbB2 inhibitor lapatinib (trade name Tykerb) was developed to combat EGFR/ErbB2 driven cancers (Guancial, Rosenberg et al. 2011). Lapatinib is another small molecule inhibitor which binds the ATP binding pocket of EGFR and ErbB2, and

was tested in a Phase II clinical trial with unremarkable results (Wulfing, Machiels et al. 2009). While ErbB inhibitors were used in Phase II clinical trials both before and after platinum-based chemotherapy was delivered, the response rate of the tumors to lapatinib therapy has been modest (Zachos, Konstantinopoulos et al. 2010). This is in spite of strong EGFR and/or ErbB2 expression on pretreatment biopsies (Mooso, Vinall et al. 2014). Although newer trials utilizing EGFR and ErbB2 inhibitors continue, taken together, the results described to date, point to a need for a better understanding of why EGFR-based therapies do not work appreciably *in vivo*.

Previous studies from lung and related cancers have shown that resistance to ErbB inhibitors may result from an upregulation of ErbB3 expression. This would supply extra binding partners for ErbB2 and ErbB4, thus circumventing a cellular need for EGFR signaling (Engelman, Zejnullahu et al. 2007). EGFR, ErbB3, and ErbB4, but not ErbB2, have known ligands. EGF serves as the ligand for EGFR, while the heregulins 1 and 2 (HRG1&2) are the ligands for ErbB3. Similarly, HRG 3&4 serve as the ligands for ErbB4 (Olayioye, Neve et al. 2000). However, ErbB3 lacks significant kinase activity (Jathal, Chen et al. 2011). Thus, ErbB2 and ErbB3 require heterodimerization for phosphorylation and activation. Therefore, it is reasonable to think that the inhibition of EGFR and ErbB2 has been ineffective due to the sustained activity of ErbB3. By leaving ErbB3 uninhibited it can dimerize with ErbB4, and thus propagate EGFR family signaling. It was previously shown in prostate cancer cells that

sustained ErbB3 activity maintained proliferation and survival, despite inhibition of either EGFR or ErbB2 (Chen, Mooso et al. 2011).

We therefore decided to investigate the potential of a novel pan-ErbB inhibitor, dacomitinib (PF00299804), which has been shown to inhibit EGFR, ErbB2 and ErbB4. Dacomitinib works by binding the kinase domain of each molecule, thus preventing their phosphorylation and activation (Engelman, Zejnullahu et al. 2007). It is believed that the addition of this drug to a regimen of platinum-based chemotherapy will enhance the tumor-specific cytotoxicity of the regimen by blocking mitosis of the ErbB over-expressing tumor cells, both mechanically and chemically.

Hypothesis and Objectives

The hypothesis for this study is that resistance to platinum-based therapies in bladder cancer concurrently confers resistance to ErbB inhibitors in bladder cancer cell lines. The two objectives for this study were: (1) to determine the mechanism by which cisplatin affects the ErbB pathway in bladder cancer cell lines and (2) to determine if ErbB inhibitors sensitize bladder cancer cells to cisplatin.

METHODS

The experiments detailed in this thesis were conducted at the VA Medical Center in Sacramento, CA. All experiments were conducted in the laboratory of Dr. Paramita Ghosh, under her supervision, between September 2012 and September 2014. This material is the result of work that was supported by resources from the VA Northern California Health Care System, Sacramento, California.

Cell Lines and Reagents Used in this Study

T24, TCCSUP, J82, and RT4 cell lines were purchased from American Type Culture Collection (ATCC, Manassas, VA). Characteristics of these cell lines are presented in Table 1 and have been previously described (Rigby and Franks 1970, Bubenik, Baresova et al. 1973, Nayak, O'Toole et al. 1977, O'Toole, Price et al. 1978)**.** In general, cells were grown in RPMI 1640 (Invitrogen, Grand Island, NY) supplemented with 10% fetal bovine serum (FBS; Gemini Bio Products, West Sacramento, CA) and 1% Penicillin/Streptomycin (Invitrogen, Grand Island, NY) unless otherwise indicated. Cycloheximide (Sigma-Aldrich, St. Louis, MO) was used at a final concentration of 100 µg/ml in all experiments for the duration indicated. Epidermal growth factor (EGF) was used to stimulate cells for 15 minutes at a final concentration of 10 ng/ml. Heregulin (HRG) was used to stimulate cells for 30 minutes at a final concentration of 50 ng/ml.

Cell Line	Tumor Stage/Grade	Age	Gender	Ethnicity	Treatment	Metastases	References
T24	Grade 3	81	Female	Caucasian	Electro-coagulation	Unknown	Bubenik, Baresova, et al. 1973
TCCSUP	Grade 4	67	Female	Unknown	None	Metastases to bone marrow	Nayak, O'Toole et al. 1977
J82	T3	58	Male	Caucasian	None	None	O'Toole, Price et al. 1978
RT4	T2a	63	Male	Caucasian	Diathermy and gold grain insertion	Unknown	Rigby and Franks 1970

Table 1. Characteristics of urinary bladder epithelial cells taken from patients with TCC used in this study. Characteristic information was collected from each of the primary research articles in which these cell lines were first described.

Pharmacologic Treatments Used to Inhibit the ErbB Family

Tarceva and lapatinib were purchased from LC Labs (Woburn, MA). Dacomitinib was purchased from Sellek Chemicals (Houston, TX). Cisplatin was purchased from Fisher Scientific (Waltham, MA). Trastuzumab was obtained from the pharmacy of the Comprehensive Cancer Center at the University of California, Davis Medical Center (Sacramento, CA). Tarceva, lapatinib, and dacomitinib were dissolved in dimethylsulfoxide (DMSO). Cisplatin was dissolved in a platinum binding buffer (3 mM NaCl and 1 mM sodium phosphate). Trastuzumab came prepared in a proprietary buffer supplied by the manufacturer.

Primary Antibodies Used in Western Blot Detection

The following primary antibodies were purchased from Cell Signaling Technology (Danvers, MA): t-EGFR, p-EGFR(T669), p-EGFR(Y845), p-EGFR(Y992), p-EGFR(Y1045), p-EGFR(Y1068), p-EGFR(Y1086), p-ErbB2(Y877), p-ErbB2(Y1196), p-ErbB2(Y1248), t-ErbB3, p-ErbB3(Y1197), p-ErbB3(Y1289), p-ErbB3(Y1328), p-ERK1/2, and α-Tubulin. The GAPDH primary antibody was purchased from Millipore (Billerica, MA), while the t-ErbB2 antibody was purchased from Santa Cruz Biotechnology (Santa Cruz, CA).

Transfection of siRNA to Knockdown the ErbB Family

For this study, siRNAs against EGFR, ErbB2 and ErbB3 as well as a non-specific scrambled control siRNA were purchased from Santa Cruz Biotechnology (Santa Cruz, CA). The indicated amount of siRNA was incubated for two minutes in 250 µl of serum-free RPMI 1640 medium supplemented with 1% Penicillin/Streptomycin (Invitrogen, Grand Island, NY) in a polypropylene 15 ml tube. In a separate tube, 5 µl of Lipofectamine 2000 (Invitrogen, Grand Island, NY) was incubated for two minutes in 250 µl of serum-free RPMI 1640 medium supplemented with 1% Penicillin/Streptomycin (Invitrogen, Grand Island, NY). Following a two minute incubation, the Lipofectamine/media mixture was added to the siRNA/media mixture and incubated for 15 minutes. During the 15 minute incubation, the cells were washed once with 5 ml of PBS and then allowed to sit in 2 ml of serum-free RPMI 1640 medium supplemented with 1% Penicillin/Streptomycin. After the 15 minute incubation, the Lipofectamine/siRNA/media mixture was added to the cells and cells were incubated at 37^{o}C for four hours in a 5% CO_2 incubator at 70% relative humidity. After four hours, 2.5 ml of RPMI 1640 supplemented with 20% FBS (Gemini Bio Products, West Sacramento, CA) and 1% Penicillin/Streptomycin was added to the cells. Sequences of all siRNA molecules used in this study can be found in Table 2.

siRNA	Strand	Sequence
Control	Sense	5’-UUC UCC GAA CGU GUC ACG U-3’
Control	Antisense	5’-ACG UGA CAC GUU CGG AGA A-3’
EGFR	Sense	5’-CUC UGG AGG AAA AGA AAG U-3’
EGFR	Antisense	5’-ACU UUC UUU UCC UCC AGA G-3’
ErbB2	Sense	5’-GGG AAA CCU GGA ACU CAC CUA CTT-3’
ErbB2	Antisense	5’-GUA GGU GAG UUC CAG GUU UCC CTT-3’
ErbB3	Sense	5’-CCA AUA CCA GAC ACU GUA CTT-3’
ErbB3	Antisense	5’-GUA CAG UGU CUG GUA UUG GTT-3’

Table 2. Sequences of the siRNA molecules used for protein knockdown. All siRNA molecules were obtained from Santa Cruz Biotechnology, Santa Cruz, CA.

Western Blot to Determine Protein Concentration and Activation

After receiving the indicated treatment, cells were washed twice with PBS to remove media and any treatment. Cells were then lysed on ice using 300 µl of 1X Sample Buffer (3.75 mM Tris HCl, pH 8.8, 10% Glycerol and 2.5% Sodium Dodecyl Sulfate). Protein concentrations for each sample were determined by bicinchoninic acid (BCA) assay (Pierce, Rockford, IL) and standardized against a set of bovine serum albumin (BSA) standards. Using protein concentrations from this assay, 50 µg of protein from each sample was loaded onto SDS-polyacrylamide gels. These gels were then run using a Mini-Protean 3 Electrophoresis Cell (Bio-Rad, Hercules, CA) at 150V. Following the run, the proteins were transferred to a 0.2 µm polyvinylidene difluoride membrane (Life Technologies, Grand Island, NY) at 20V for 10 minutes using an iBlot Transfer Device (Life Technologies, Grand Island, NY). After transfer, membranes were blocked for one hour with a 5% milk solution made in TBS-T (50 mM Tris HCl, pH 7.6, 150 mM NaCl, 0.1% Tween 20). This procedure was done in an effort to prevent non-specific binding of the primary and secondary antibodies. Membranes were then washed three times with TBS-T for five minutes per wash and then incubated with primary antibody overnight at 4^{o}C with shaking. Primary antibody was prepared at a dilution of 1:500 in a 1% BSA solution. Membranes were next washed three more times in TBS-T for five minutes per wash. Following sufficient washing, the membranes were then incubated with Rabbit anti-mouse IgG or Goat anti-rabbit IgG (Jackson Immunoresearch, West Grove, PA) for one hour at room temperature with

shaking. The anti-mouse secondary antibody was prepared at a concentration of 1:3000 and was only used for detection of GAPDH. The anti-rabbit secondary antibody was prepared at a concentration of 1:5000 and was used for detection of the remaining proteins. Both secondary antibodies were conjugated to horseradish peroxidase to allow for detection. Following secondary antibody application, membranes were washed five times for five minutes per wash in TBS-T, and then incubated with Super Signal West Femto chemi-luminescent substrate (Pierce, Rockford, IL) for two minutes. The chemi-luminescent substrate was diluted in de-ionized water at a dilution of 1:20. Membranes were visualized using autoradiography film and developed using an automated developing system.

Flow Cytometry to Determine Change in Apoptosis

Cells were trypsinized and collected in individual 15 ml centrifuge tubes with 5 ml of FBS containing medium. Cells were then collected by centrifugation at 200 g in a bench-top 4^{o}C centrifuge (Eppendorf 5417R) for four minutes. The supernatant was aspirated and each pellet was washed with 1 ml of PBS. Cell pellets were collected again by centrifugation at 200g for four minutes at 4^{o}C. Cells were then resuspended in 360 µl of 1X Annexin Binding Buffer (Invitrogen, Grand Island, NY). Cells were stained by using 10 µl of 100 µg/ml propidium iodide (Invitrogen, Grand Island, NY) and 1 µl Annexin V-Alexa Fluor 647 (Invitrogen, Grand Island, NY). Data were collected using a BD FACSCalibur flow cytometer (Becton Dickinson

Immunocytometry Systems, San Jose, CA). Cells were illuminated with 200 mW of 488 nm light produced by an argon-ion laser and 635 nm light produced by a red-diode laser. Fluorescence of propidium iodide was read through a 630/22 nm band-pass filter, while fluorescence of AlexaFluor 647 was read through a 661/16 nm band-pass filter. Data were collected on 20,000 cells as determined by forward and right-angle light scatter, and stored as frequency histograms. Determination of percent of cells actively undergoing apoptosis was made by analyzing the collected data using Cell Quest (Becton Dickinson Immunocytometry Systems, San Jose, CA). Cells which failed to exclude the DNA intercalating agent propidium iodide were considered to be damaged or necrotic. Meanwhile, cells which bound the Annexin V-Alexa Fluor 647 were determined to be apoptotic, as expression of Annexin V on the cell surface is a marker of apoptosis (Koopman, Reutelingsperger et al. 1994).

Flow Cytometry to Determine Accumulation of Cells in Each of the Cell Cycle Phases

Flow cytometry was performed to determine the percent of cells in each phase of the cell cycle. Cells were trypsinized and collected in individual 15 ml centrifuge tubes with 5 ml of FBS containing medium. Cells were then collected by centrifugation at 200 g in a bench-top 4^{o}C centrifuge (Eppendorf 5417R) for four minutes. The supernatant was aspirated and each pellet was washed with 1 ml of PBS. Cell pellets were collected again by centrifugation at 200 g for four minutes at 4^{o}C. Cells were resuspended in 1 ml of -20^{o}C 70% ethanol. Following resuspension, cells were fixed by

incubation in a -20^{o}C freezer for four hours, which allowed the propidium iodide to enter the nuclei and bind to the DNA. After incubation, the cells were removed from the freezer and collected by centrifugation at 200 g for four minutes at 4^{o}C. The supernatant was aspirated and the pellets were washed in 1 ml of PBS. Cell pellets were recollected by centrifugation at 200 g for four minutes at 4^{o}C. The cells were resuspended in PBS containing 1% BSA at 4^{o}C to block. After blocking, the cells were collected by centrifugation at 200 g at 4^{o}C for four minutes and the supernatant was aspirated. The cells were then resuspended in 260 µl of a PBS solution containing 5 µl of 10 mg/ml RNase A (Roche, Basel, Switzerland) and 10 µl of 50 µg/ml propidium iodide (Invitrogen). Data were collected using a BD FACSCalibur flow cytometer (Becton Dickinson Immunocytometry Systems, San Jose, CA). Cells were illuminated with 200 mW of 488 nm light produced by an argon-ion laser. Fluorescence was read through a 630/22 nm band-pass filter. Data were collected on 20,000 cells as determined by forward and right-angle light scatter and stored as frequency histograms. Determination of percent of cells in each phase of the cell cycle was made by analyzing the collected data using MODFIT (Verity software, Topsham, ME). Flow cytometry measured the relative amount of propidium iodide in each cell. Cells with approximately a 1X concentration of propidium iodide were considered to be in the G1/G0 phase of the cell cycle. Similarly, cells with an approximately 2X concentration were determined to be in the G2/M phase of the cell cycle. In contrast, cells with a 1-

2X concentration of propidium iodide were determined to be in the S phase of the cell cycle (Moore, Donahue et al. 1998).

MTT Assay to Determine Growth Retardation of Treatments

The mitochondrial activity of treated cells was assessed as follows. Cells were plated into each well of a 24-well multi-plate. T24 cells were plated at a density of $1.5*10^3$ cells per well, while the other cell lines were all plated at a density of $3*10^3$ cells per well. All cells were plated in FBS containing medium. For each treatment, three plates were plated and an additional fourth plate was plated for a Day 0 baseline control. The plates were incubated at 37^{o}C for 24 hours in a 5% CO_2 incubator at 70% relative humidity. After incubation, the cells were treated in triplicate as indicated. Cells were allowed to grow in treatment for up to five days. On the same day as treatment, the Day 0 plate was incubated with 125 µg of 3-[4,5-Dimethylthiazol-2yl]-2,5-diphenyl-tetrazolium bromide (MTT) (Sigma-Aldrich, St. Louis, MO) in each well. On days 1, 3 and 5, each well of the appropriate plate was treated with 125 µg of MTT reagent. The plate was then incubated at 37^{o}C in a 5% CO_2 incubator at 70% relative humidity for one hour. After the incubation, the MTT reagent and media were aspirated from each well and replaced with 500 µl of DMSO (Sigma-Aldrich, St. Louis, MO). The addition of the DMSO helped to permeabilize the cells and release the formazan which had been formed. The plate was then incubated on a rocker for 10 minutes. After incubation, 200 µl of the DMSO and formazan mixture was transferred from each well

to a 96-well multiplate. The 96-well plate was then read by a Power Wave spectrophotometer (Bio-Tek Instruments, Burlington, VT) at 562 nm.

Reverse Transcriptase Quantitative PCR to Determine ErbB3 Knockdown

Cells were transfected with the siRNA as previously indicated and incubated for 72 hours at 37^{o}C in a 5% CO_2 incubator at 70% relative humidity. Cellular RNA was then extracted and collected using an RNeasy MiniKit (Qiagen, Valencia, CA). Total RNA concentration and quality was determined using a NanoDrop spectrophotometer (Thermo Scientific, Waltham, MA). Synthesis of cDNA was performed using a Revert-Aid First Strand Synthesis cDNA kit (Thermo Scientific, Waltham, MA) using 100 ng of total RNA and an Oligo-dT^{18} primer. Use of this primer was employed to select for mRNA in the cDNA synthesis process. After cDNA synthesis, single-stranded DNA concentration and quality was determined using a NanoDrop spectrophotometer. Reverse transcriptase quantitative PCR (RT qPCR) was performed on a StepOne Plus Thermal Cycler (Applied Biosystems, Grand Island, NY). RT qPCR was carried out using the Luminaris HiGreen High ROX qPCR Master Mix (Thermo Scientific, Waltham, MA) and 200 ng of cDNA template. Sequences of the β-actin and ErbB3 primers are given in Table 3. The β-Actin (O'Reilly, Kosaka et al. 2001) and ErbB3 (Bieche, Onody et al. 2003) primers were taken from the literature. These primers were

Gene	Primer	Sequence	Reference
β-Actin	Forward	5’- TCA CCC ACA CTG TGC CCA TCT ACG A-3’	O’Reilly, Kosaka et al. 2001
β-Actin	Reverse	5’- CAG CGG AAC CGC TCA TTG CCA ATG G-3’	O’Reilly, Kosaka et al. 2001
ErbB3	Forward	5’- GTC TGT GTG ACC CAC TGC AAC T-3’	Bieche, Onody et al. 2003, Gunes, Sullu et al. 2013
ErbB3	Reverse	5’- GGG TGG CAG GAG AAG CAT T-3’	Bieche, Onody et al. 2003, Gunes, Sullu et al. 2013

Table 3. Sequences of the primers used for RT qPCR analysis.

later validated for use in bladder cancer and with SYBR green reagents (Gunes, Sullu et al. 2013).

Cycloheximide Assay to Determine ErbB3 Protein Stability

Cells were plated into 100 mm dishes at a density of $2*10^6$ and grown in 10 ml of RPMI 1640 supplemented with 10% FBS and 1% Penicillin/Streptomycin until confluent at 37^{o}C in a 5% CO_2 incubator at 70% relative humidity. Upon reaching confluency, the media was spiked with 1 mg of cycloheximide and the cells were further incubated at 37^{o}C in a 5% CO_2 incubator at 70% relative humidity until reaching the indicated time point. Upon reaching the indicated time point, the media and cycloheximide were aspirated from the dish, and the cells were washed twice with PBS. Cells were then frozen at -80^{o}C until they could be prepared for Western Blotting.

Statistical Analysis to Objectively Measure Treatment Effects

Statistical analysis was performed using GraphPad Prism 6 software (La Jolla, CA). All analyses were performed using at least three biologic replicates and one- or two-way ANOVA with *post-hoc* multiple comparisons. All data are represented as the mean of the replicates ± standard deviation.

RESULTS

Overexpression of the EGFR Family in Bladder Cancer

Overexpression of the EGFR family in bladder cancer is well documented in the literature (Rajkumar, Stamp et al. 1996, Chow, Liu et al. 1997, Chow, Chan et al. 2001, Rotterud, Nesland et al. 2005, Amsellem-Ouazana, Bièche et al. 2006, Chaux, Cohen et al. 2012). To ensure that the cells used in this work were representative of the cases reported in the literature, the T24, TCCSUP, J82 and RT4 cells were probed via Western blotting for expression of EGFR, ErbB2, ErbB3, and ErbB4 as shown in Figure 2. These cells were run alongside the prostate cancer C4-2 cells (Wu, Hsieh et al. 1994) and MCF7 breast cancer cells (Soule, Vazguez et al. 1973) for which the levels of EGFR family expression are well known. As shown, the T24, TCCSUP, and J82 cell lines all overexpressed EGFR and ErbB3 when compared to C4-2 or MCF7 cells. In addition, these three cell lines produced similar levels of ErbB2 when compared to the MCF7 cell line which does not overexpress ErbB2 (Soule, Vazguez et al. 1973). All three cell lines produced low levels of ErbB4, characteristic of bladder cancer cells (Junttila, Laato et al. 2003). On the other hand, the RT4 cell line expressed only low levels of EGFR, and expressed lower levels of ErbB2, ErbB3, and ErbB4 when compared to MCF7 cells.

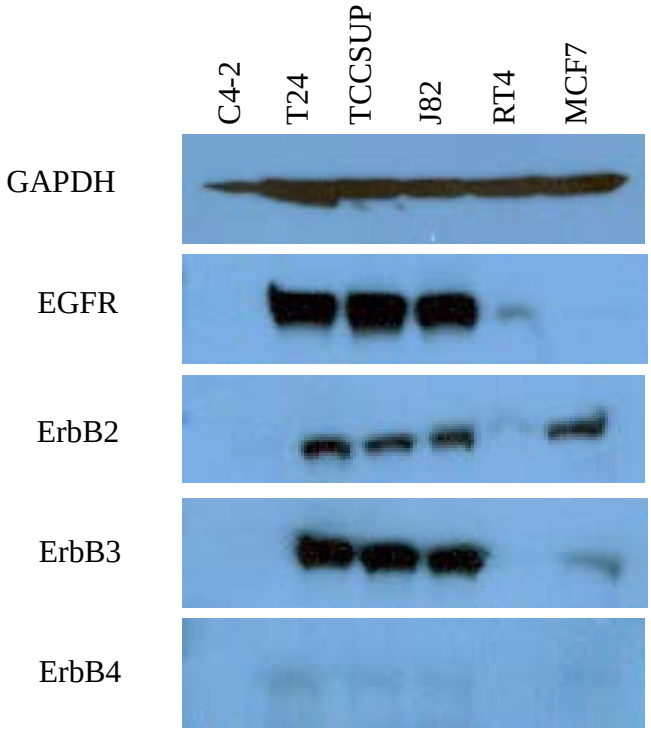

Figure 2. Relative expression of the EGFR family of receptors in eukaryotic cell lines used in this study. Lysate preparations of the four bladder cancer cells lines T24, TCCSUP, J82 and RT4 were run on polyacrylamide gels alongside the C4-2 and MCF7 cell lines. Western blots were probed for EGFR, ErbB2, ErbB3, and ErbB4 to show relative expression of these proteins. Constitutively expressed GADPH was used as a loading control.

Cisplatin Sensitivity of Bladder Cancer Cells

MTT assay, which measures the mitochondrial activity of cells, was employed to determine the relative sensitivity of each of the four cell lines to treatment with cisplatin. Table 4 shows the dose response curve of each cell line when treated with increasing doses of cisplatin. The optical density on day 5 of treatment represents the concentration of MTT reagent converted to formazan by the mitochondria of living cells. Since dividing cells have increased mitochondrial activity when compared to quiescent cells, the majority of the formazan is produced by dividing cells. Meanwhile, a basal level of formazan is still created by the quiescent cells. Based on the observed responses, the dose of cisplatin at which half of the cells cease to proliferate (IC_{50}) was determined by dose-response curve-fitting using GraphPad. J82 cells were determined to be the most sensitive to cisplatin treatment as observed by the dose response curve dipping earlier than the other three cell lines. The remaining cell lines were determined to be resistant to cisplatin treatment. Owing to these results, and physiologically attainable serum levels previously reported (Royer, Delroeux et al. 2008), a concentration of 200 nM cisplatin was used for the remainder of the experiments in this study.

Cell Line	IC_{50}
T24	119.9 nM (114.6 – 125.4)‡
TCCSUP	224.7 nM (212.5 – 237.6)
J82	65.2 nM (41.6 – 102.2)
RT4	244.1 nM (162.4 – 366.7)

Table 4. Relative cisplatin sensitivity of bladder cancer cell lines used in this study. IC_{50} values are given for each of the four cell lines following treatment with varying concentrations of cisplatin, and subsequent curve fitting in GraphPad. ‡ 95% Confidence Interval

Knockdown of the EGFR Family Causes Cisplatin-Induced Growth Retardation

Small-interfering RNAs (siRNAs) against EGFR, ErbB2, and ErbB3 were employed to determine what effect lowering the expression of these proteins would have on the cells. Western blotting was used to visualize the knockdown of the target protein while MTT assays were used to determine growth retardation. Flow cytometry was employed to determine relative apoptosis and cell cycle progression as previously described. Figures 3 and 4 demonstrate the validation of the EGFR siRNA, and growth inhibitory effects of the EGFR siRNA, respectively. Figures 5 and 6 demonstrate the validation of the ErbB2 siRNA, and effects of ErbB2 siRNA on growth, respectively. Figures 7, 8, and 9 demonstrate the effects of both siRNAs in combination with cisplatin treatment. Figure 7 demonstrates the effects on apoptosis of bladder cancer cells while Figures 8 and 9 demonstrate the effects on cell cycle distribution of bladder cancer cells. Figure 10 shows the inefficacy of the ErbB3 siRNA in knocking down ErbB3 expression in T24, TCCSUP, and RT4 cell lines. Figure 11 demonstrates the effect of ErbB3 siRNA on ErbB3 mRNA levels. Figure 12 shows the half-life of the ErbB3 protein molecule in each cell line. Figure 13 shows the effect of ErbB3 siRNA on the growth of the J82 cell line. Figures 14 and 15 show the effect of ErbB3 siRNA on the cell cycle distribution, and rate of apoptosis in the J82 cell line, respectively, when used with or without cisplatin.

The EGFR siRNA was able to induce knockdown of EGFR protein levels in all cell lines (Figure 3). Furthermore, EGFR knockdown led to a statistically significant

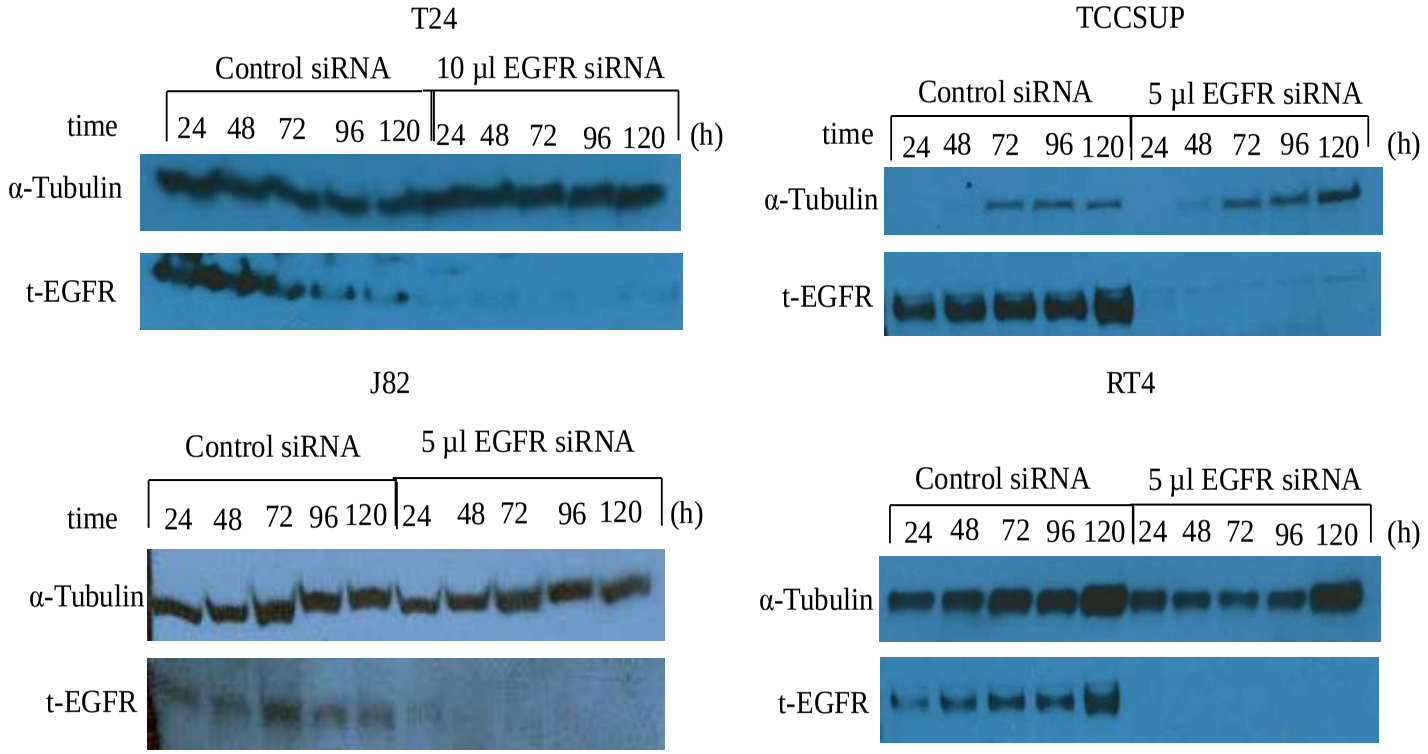

Figure 3. Evidence of *in vitro* EGFR gene expression knockdown in T24, TCCSUP, J82 and RT4 cells with EGFR siRNA. Western blot results of samples taken on consecutive days after treatment with a scrambled siRNA sequence (Control) or treatment with EGFR siRNA. Blots were normalized to α-tubulin.

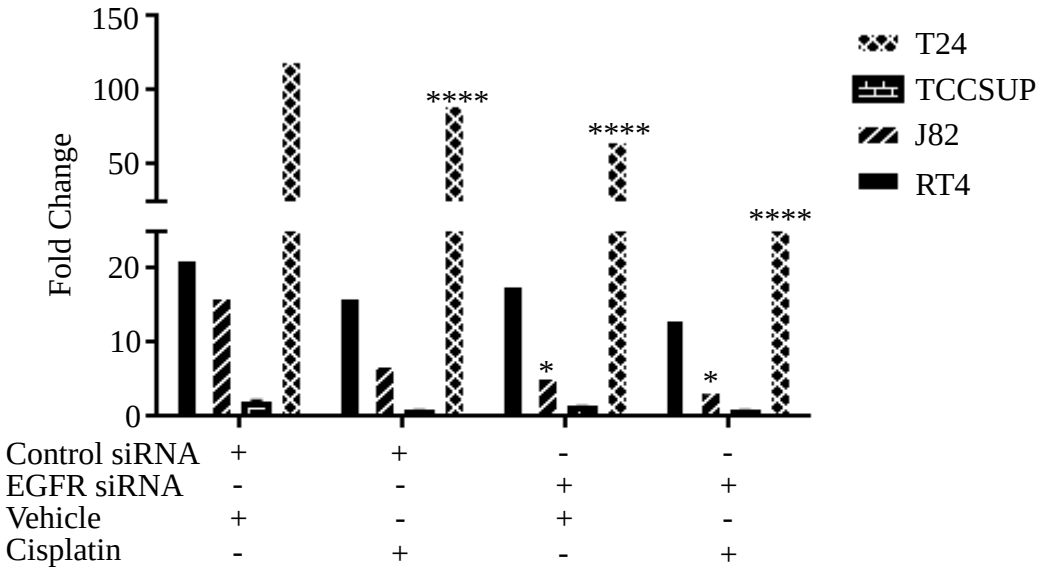

Figure 4. EGFR siRNA and cisplatin induced growth retardation. MTT assays showing growth retardation effects of EGFR siRNA and cisplatin alone or in combination on Day 5 of treatment. Each bar in the graph represents the average of the results obtained from three independent experiments ± standard deviation. Significance indicators show the relation between the indicated treatment and the "Control siRNA Vehicle" treatment. * = p-value < 0.05, **** = p-value < 0.0001

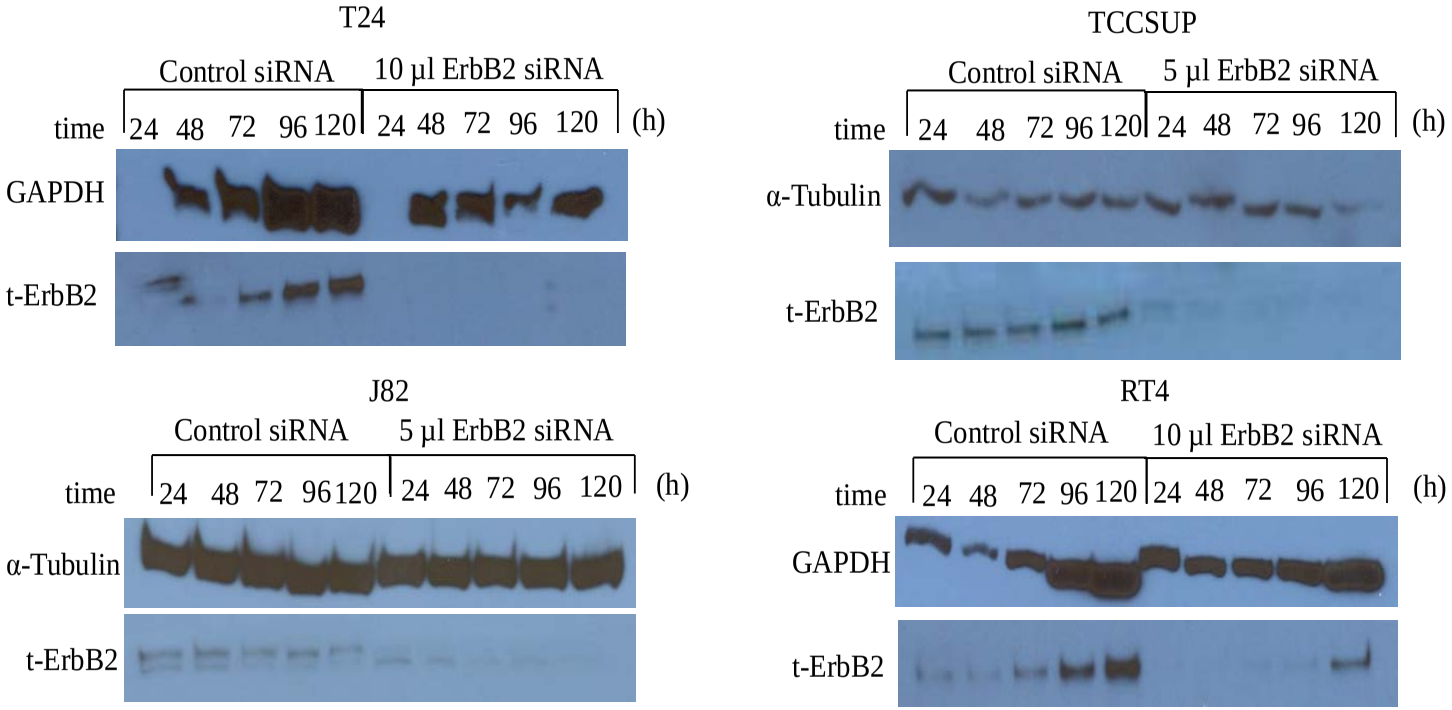

Figure 5. Evidence of *in vitro* ErbB2 gene expression knockdown in T24, TCCSUP, J82 and RT4 cells with ErbB2 siRNA. Western blot results of samples taken on consecutive days after treatment with a scrambled siRNA sequence (Control) or treatment with ErbB2 siRNA. Blots were normalized to α-tubulin or GAPDH.

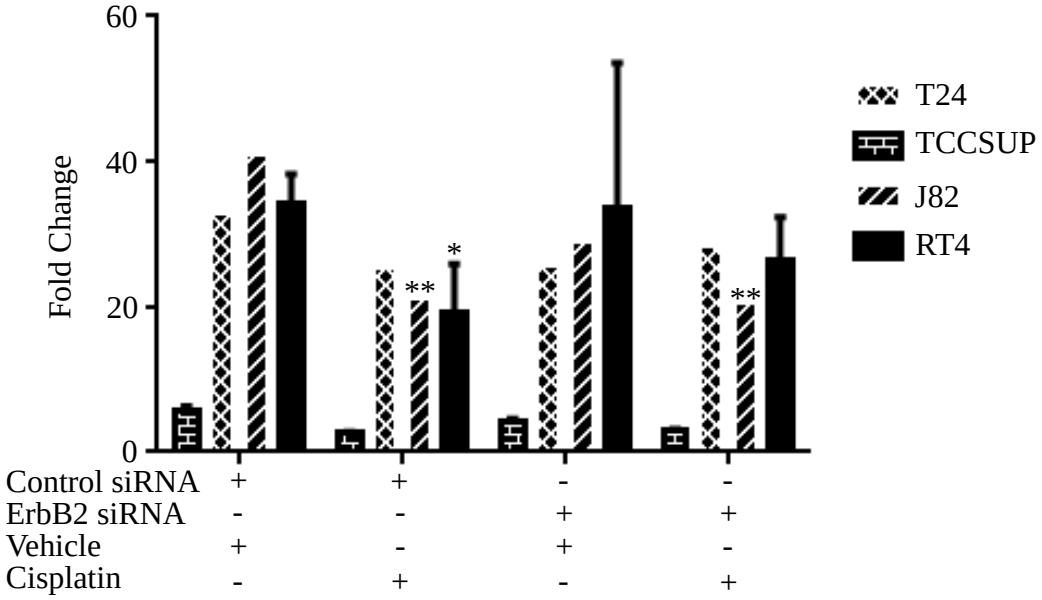

Figure 6. ErbB2 siRNA and cisplatin induced growth retardation. MTT assays showing growth retardation effects of ErbB2 siRNA and cisplatin alone or in combination on Day 5 of treatment. Each bar in the graph represents the average of the results obtained from three independent experiments ± standard deviation. Significance indicators show the relation between the indicated treatment and the "Control siRNA Vehicle" treatment. * = p-value < 0.05, ** = p-value < 0.01

decrease in cellular growth when compared to cells transfected with control siRNA and treated with vehicle (Figure 4). Additionally, the combination of transfection with EGFR siRNA and treatment with cisplatin was more effective at inducing growth retardation than transfection with EGFR siRNA alone (Figure 4). This effect reached the level of statistical significance in both the T24 and RT4 cell lines.

The ErbB2 siRNA was also able to knockdown expression of the ErbB2 protein in all cells tested (Figure 5); however, this effect was decidedly transient in the RT4 cells (Figure 5D). Note that by day 5, the RT4 cells were already producing higher levels of ErbB2. In contrast to the growth retardation observed in EGFR siRNA transfected cells, cisplatin-resistant cells transfected with ErbB2 siRNA did not experience any added growth inhibition when treated with cisplatin versus vehicle (Figure 6).

Interestingly, while the EGFR siRNA either alone or in combination with cisplatin was able to induce growth inhibition, it was not able to induce a significant amount of apoptosis in any cell line (Figure 7). In fact, this treatment trended toward a protective phenotype in the RT4 cell line when used in conjunction with cisplatin versus control. In contrast, the ErbB2 siRNA plus vehicle treatment was able to induce an approximately three-fold increase in apoptosis in T24 cells when compared to control (Figure 7); however, this effect was abrogated by the addition of cisplatin. Additionally, RT4 cells experienced no significant change in the accumulation of cells in any phase of the cell cycle; however, J82 cells experienced a significant G2 arrest

when transfected with either EGFR or ErbB2 siRNA and treated with cisplatin versus control (Figure 9). This was determined from the observation that there was a significant increase in the percentage of cells in the G2 phase of the cell cycle. Interestingly, both the T24 and TCCSUP cell lines exhibited a significant increase in the accumulation of cells in the S phase of the cell cycle when compared to control (Figure 8). Thus, cisplatin was able to induce growth inhibition through G2 arrest, rather than apoptosis.

ErbB3 siRNA was successful in knocking down expression of ErbB3 in J82 cells; however, knockdown of this protein was not observed in T24, TCCSUP, or RT4 cells (Figure 10). This effect persisted even when the dosage of ErbB3 siRNA was increased. The next step was to determine whether this was the result of a defect in the siRNA pathway or post-translational stability of ErbB3 in these cells. To determine this, the protein biosynthesis inhibitor cycloheximide and RT qPCR were employed. RT qPCR assays revealed that levels of ErbB3 mRNA were being decreased by treatment with ErbB3 siRNA (Figure 11).

Cycloheximide assays demonstrated the high level of ErbB3 protein stability in the TCCSUP, and RT4 cell lines when compared to J82 cells (Figure 12). Cycloheximide works by blocking the movement of tRNA molecules within the ribosome (Baliga, Pronczuk et al. 1969). This blockage results in inhibition of translational elongation, and no new proteins are able to be synthesized by the cell. While the results of this assay were not statistically significant, it did show that at eight

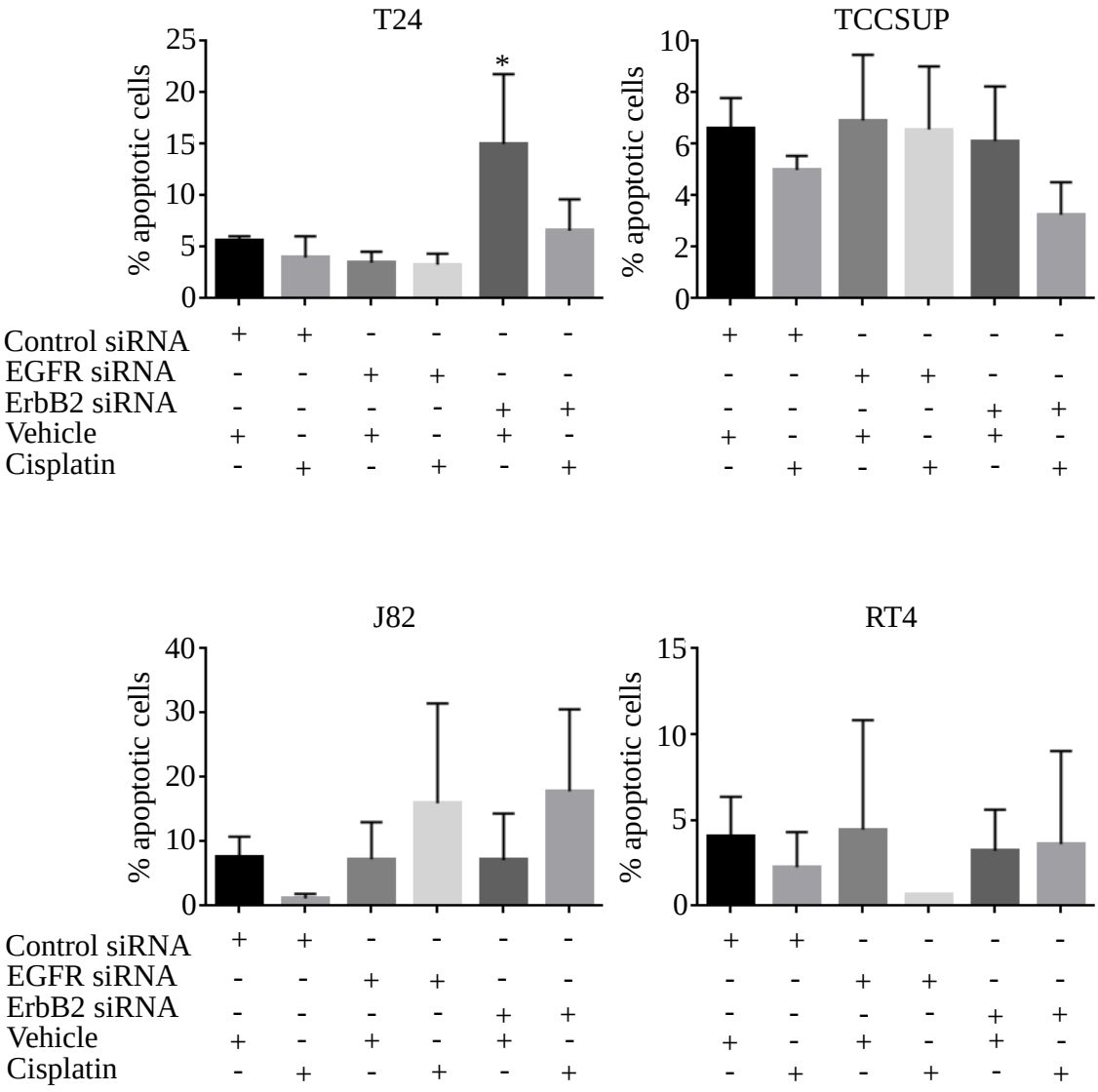

Figure 7. Apoptosis of bladder cancer cells following EGFR or ErbB2 siRNA knockdown. Cells were treated with either vehicle or cisplatin. The bars within each graph represent an average (± SD) of the results obtained from three independent experiments. Significance indicators show the relation between the indicated treatment and the "Control siRNA Vehicle" treatment. Graphs show percent of apoptosis as determined by Annexin-V staining. * = p-value < 0.05

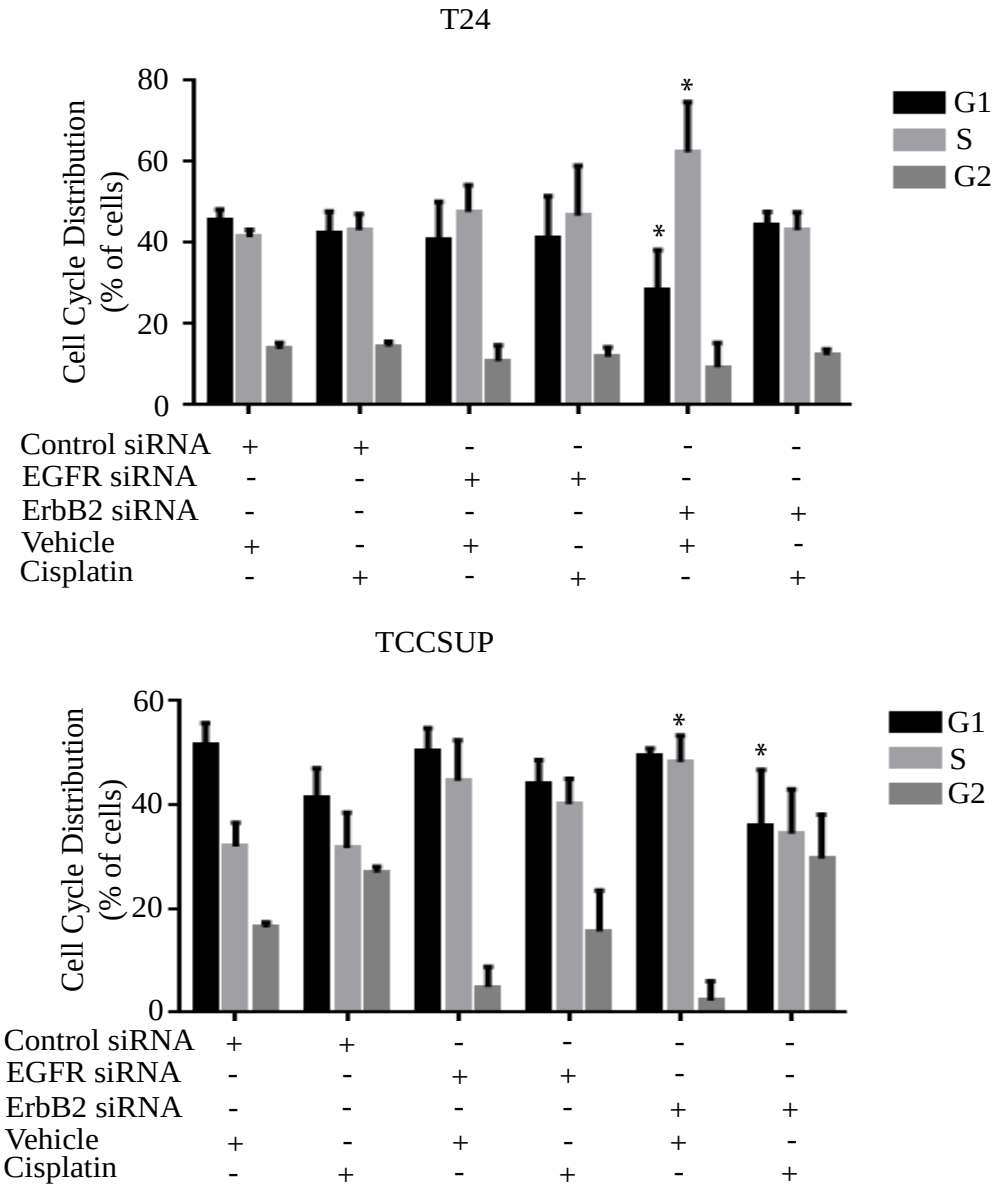

Figure 8. Cell cycle distribution of T24 and TCCSUP bladder cancer cells following EGFR or ErbB2 siRNA knockdown. Cells were treated with either vehicle or cisplatin. The bars within each graph represent an average of the results obtained from three independent experiments. Significance indicators show the relation between the indicated treatment and the "Control siRNA Vehicle" treatment. Graphs show percent of cells in each phase of the cell cycle as determined by propidium iodide staining. * = p-value < 0.05, ** = p-value < 0.01, *** = p-value < 0.001, **** = p-value < 0.0001

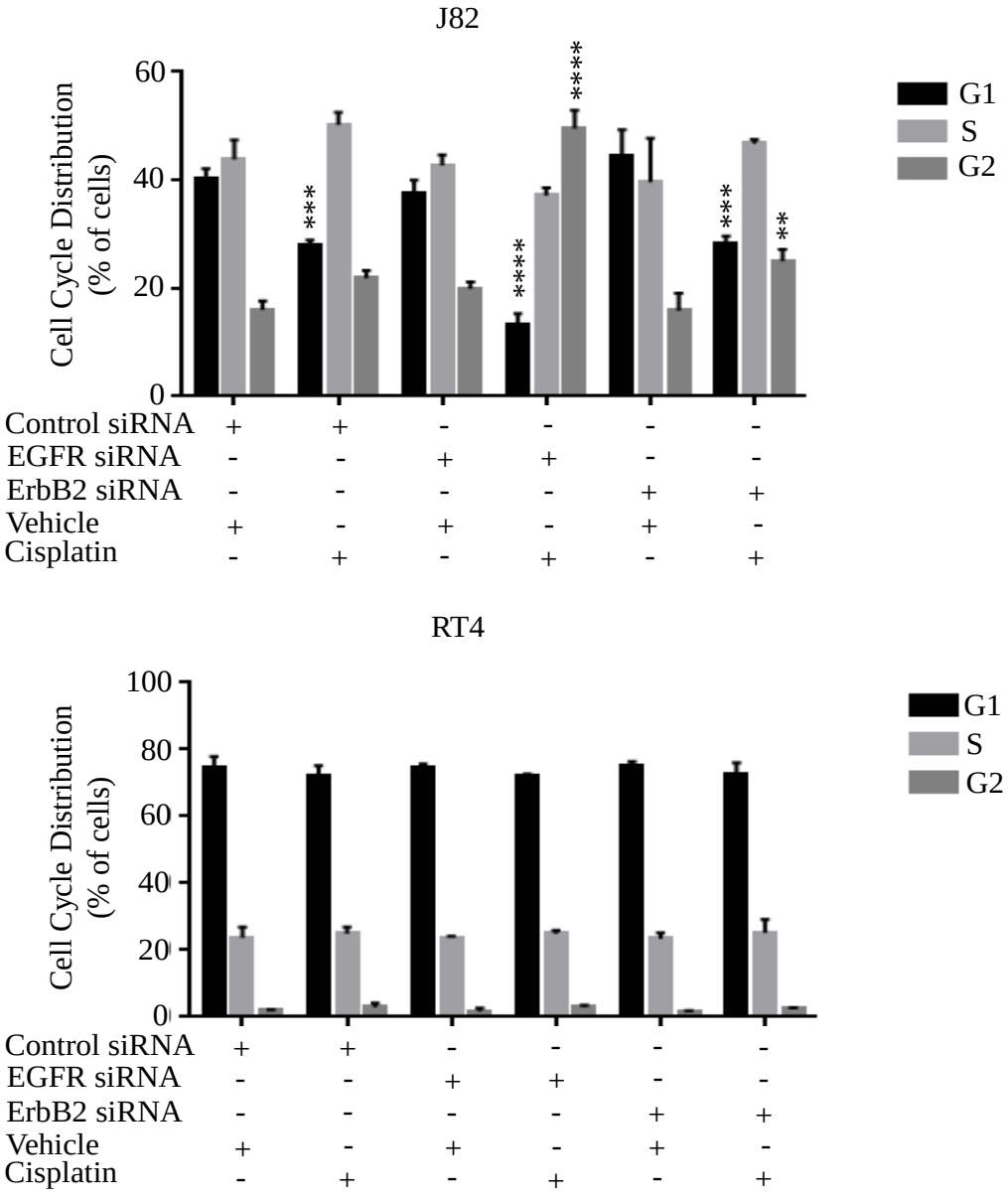

Figure 9. Cell cycle distribution of J82 and RT4 bladder cancer cells following EGFR or ErbB2 siRNA knockdown. Cells were treated with either vehicle or cisplatin. The bars within each graph represent an average of the results obtained from three independent experiments. Significance indicators show the relation between the indicated treatment and the "Control siRNA Vehicle" treatment. Graphs show percent of cells in each phase of the cell cycle as determined by propidium iodide staining. * = p-value < 0.05, ** = p-value < 0.01, *** = p-value < 0.001, **** = p-value < 0.0001

hours post cycloheximide treatment the ratio of ErbB3 to α-Tubulin had increased dramatically in the TCCSUP cell line and remained elevated even at 24 hours (Figure 12). Additionally, it was observed that at 24 hours post cycloheximide treatment the ratio of ErbB3 to α-Tubulin was steadily increasing in the RT4 and T24 cell lines (Figure 12). Meanwhile, at 24 hours post cycloheximide treatment it was observed that the ratio of ErbB3 to α-Tubulin was steadily decreasing in the J82 cell line (Figure 12). Taken together this would indicate that the half-life of ErbB3 in the T24, TCCSUP, and RT4 cell lines is all greater than that of α-Tubulin, while the half-life of ErbB3 in J82 cells is less than that of α-Tubulin, which has been shown to be stably expressed and thus have a relatively short half-life (Zhang, Tang et al. 2014). While the determination of the cause of increased ErbB3 stability in these cell lines is beyond the scope of this work, it is an interesting observation which should be investigated further.

Owing to these results, ErbB3 siRNA's effects were only investigated in the J82 cell line. In this cell line it was observed that combined treatment with ErbB3 siRNA and cisplatin reduced the growth of these cells by nearly 100% (Figure 13). Furthermore, this treatment increased the amount of cells in the G2 phase of the cell cycle by approximately 10% (Figure 14). Additionally, the combination of ErbB3 siRNA transfection and vehicle treatment caused an at least two-fold increase in levels of apoptosis when compared to control (Figure 15). However, this last observation was only a trend, as the results were not statistically significant to $p<0.05$.

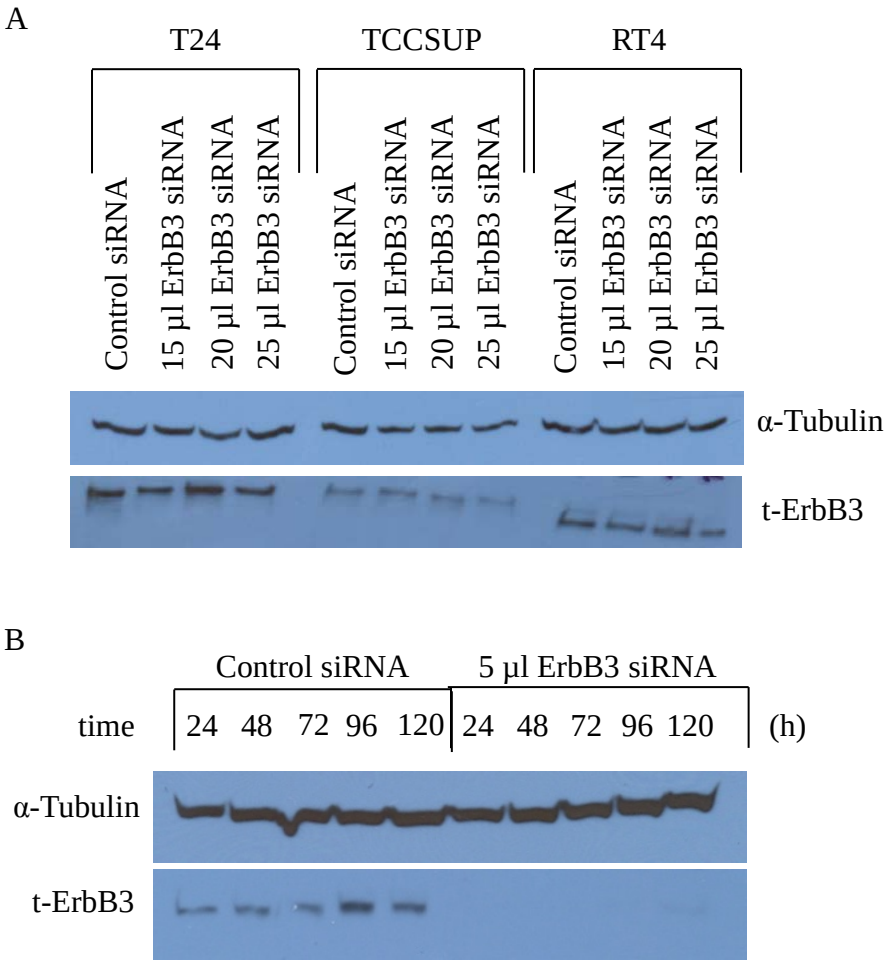

Figure 10. Evidence of *in vitro* ErbB3 gene expression knockdown in J82 cells, but not T24, TCCSUP, or RT4 cells. Blots were normalized to α-tubulin. (A) Western blots showing effect of varying amounts of ErbB3 siRNA on ErbB3 protein expression in T24, TCCSUP, and RT4 cells. (B) Western blot results of J82 samples taken on consecutive days after treatment with a scrambled siRNA sequence (Control) or treatment with ErbB3 siRNA.

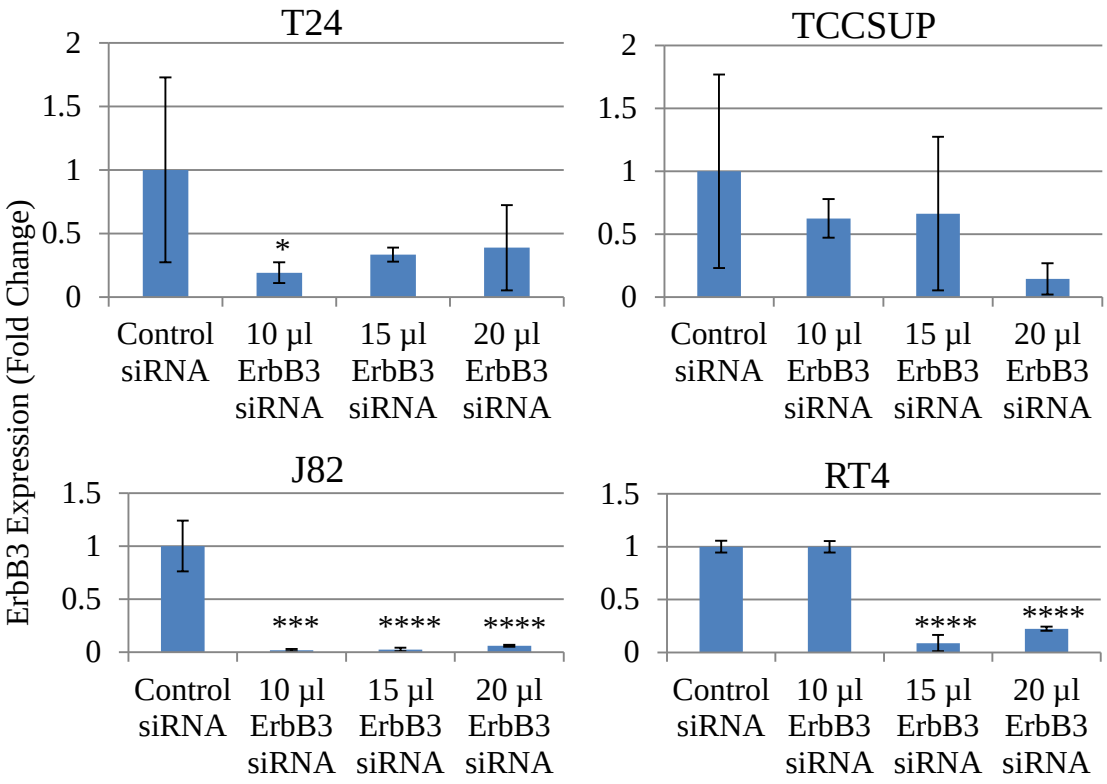

Figure 11. Evaluation of the efficacy of ErbB3 siRNA treatment. RT qPCR graphs showing relative expression of ErbB3 mRNA following treatment with the indicated siRNA. The bars within each graph represent an average of the results obtained from three independent experiments ± standard deviation. Significance indicators are all in comparison to control siRNA. * = p-value < 0.05, *** = p-value < 0.001, & **** = p-value < 0.0001

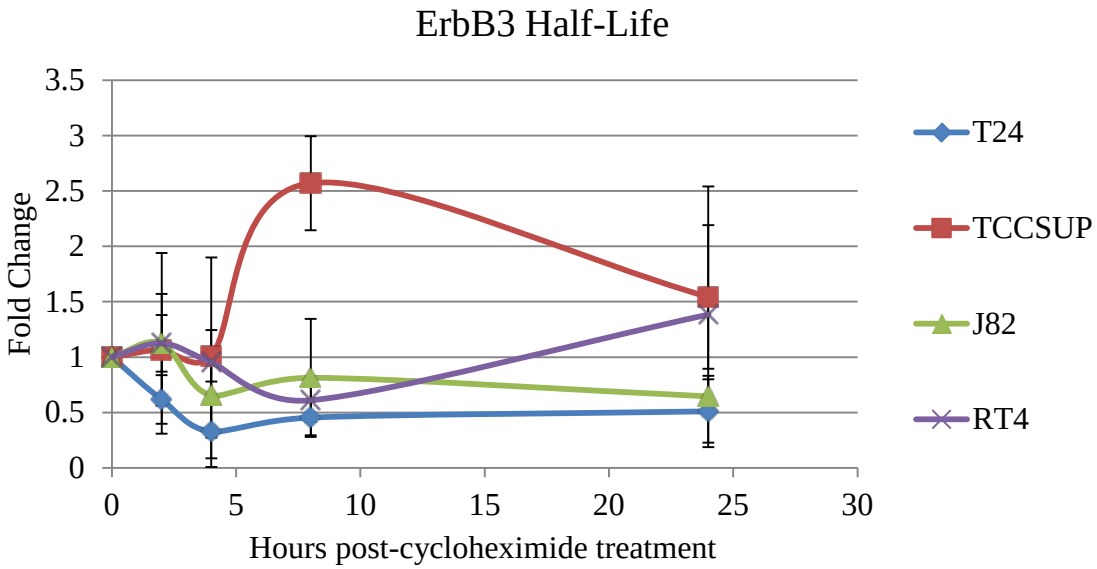

Figure 12. Analysis of ErbB3 stability in bladder cancer cells. Graph shows the relative ErbB3 expression, as compared to α-Tubulin, in the various bladder cancer cell lysates over time. Each data point represents an average of the results obtained from three independent experiments ± standard deviation.

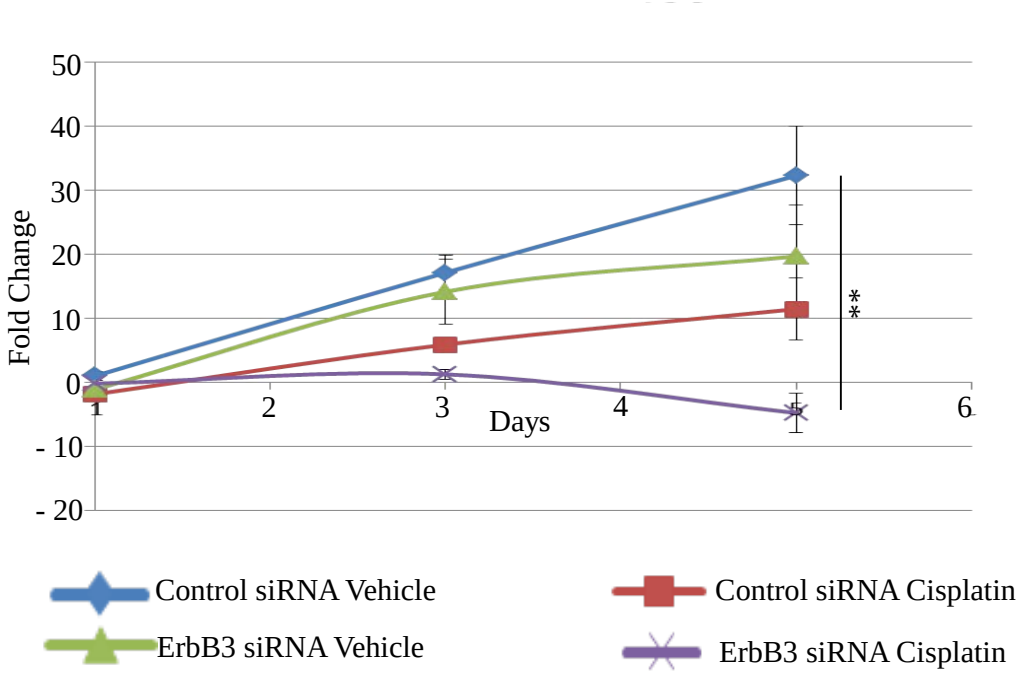

Figure 13. Effects of ErbB3 siRNA and cisplatin treatment on J82 cell growth. MTT assay showing growth retardation effects of ErbB3 siRNA and cisplatin alone or in combination. Each data point represents an average of the results obtained from three independent experiments ± standard deviation. ** = p-value < 0.01

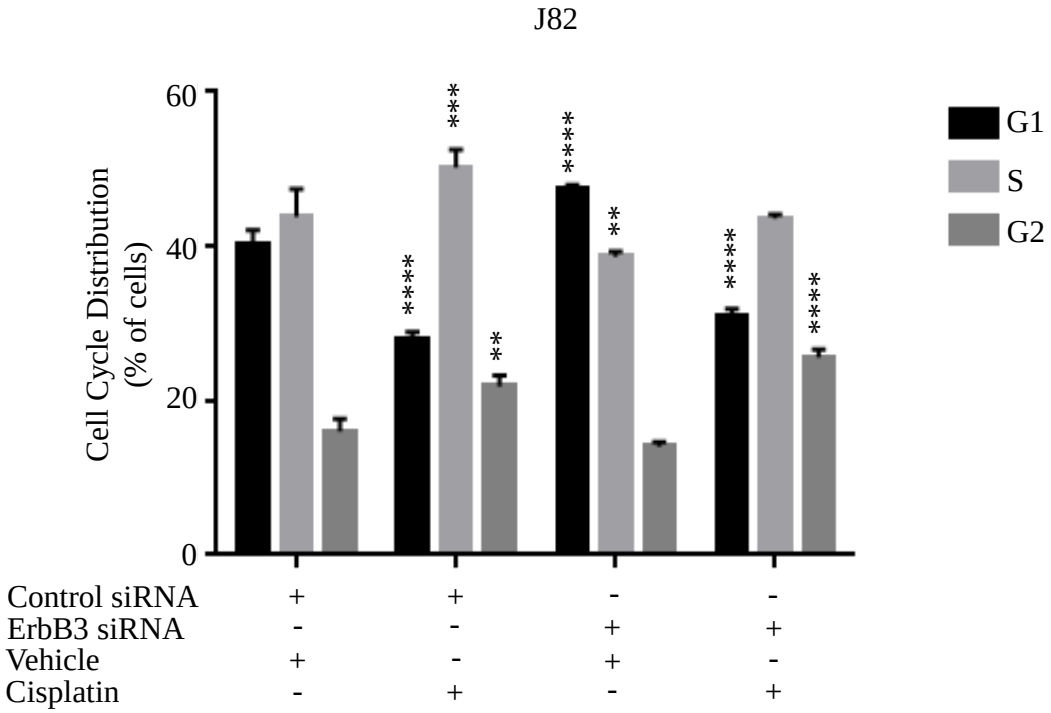

Figure 14. Effect of ErbB3 siRNA and cisplatin on cell cycle progression. Graph shows percentage of cells in the cell cycle phases as determined by propidium iodide staining and flow cytometry. The bars in the graph represent an average of the results obtained from three independent experiments. Significance indicators show the difference between the indicated treatment and the “Control siRNA Vehicle” treatment. * = p-value < 0.05 ** = p-value < 0.01, *** = p-value < 0.001, **** = p-value < 0.0001

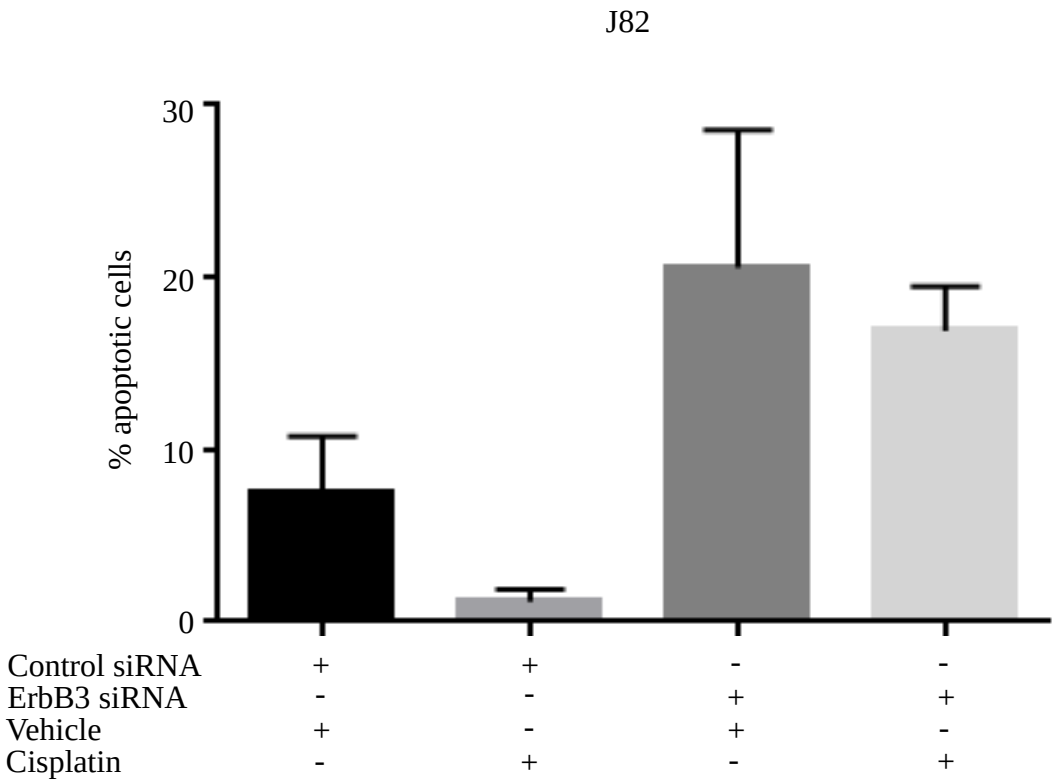

Figure 15. Effect of ErbB3 siRNA and cisplatin on apoptosis rate in J82 cells. Graph showing percentage of cells undergoing apoptosis as determined by Annexin-V staining and flow cytometry. The bars within each graph represent an average of the results obtained from three independent experiments.

Cisplatin Treatment Causes Alterations in the EGFR Family Signaling Pathway

In order to evaluate the effect of cisplatin on the EGFR family pathway, cells were treated with cisplatin for 72 hours, followed by stimulation with EGF or HRG. Western blots of lysates from treated cells were probed to evaluate the location of phosphorylation on the intracellular domain of EGFR, ErbB2, and ErbB3 as noted in the materials and methods (Figure 16). Those phosphorylation sites determined to be statistically up- or down-regulated by treatment with cisplatin are shown in Figure 17A–D. Unfortunately, no consistent pattern of the same sites being effected by cisplatin treatment was observed. However, there did seem to be a trend for the cisplatin-sensitive J82 cell line to experience a decrease in phosphorylation at EGFR tyrosine 845, a site which is known to activate the Ras pathway. Meanwhile, the cisplatin-resistant cell lines experienced an increase in phosphorylation at EGFR tyrosine 1045, tyrosine 1068, tyrosine 1086 and ErbB3 tyrosine 1197, sites known to activate the Ras pathway (Schulze, Deng et al. 2005) (Figure 16).

To determine if the Ras pathway was being affected by treatment with cisplatin, the cell lysates were probed using antibodies for phospho-ERK1/2 (Figure 17A–D). ERK1/2 was used as it is a protein kinase downstream of Ras (Kyriakis, App et al. 1992, Leevers and Marshall 1992), and serves as a reporter for Ras pathway activation. However, significant up- or down-regulation was observed for phospho-ERK1/2 in only the T24 and J82 cell lines (Figure 16).

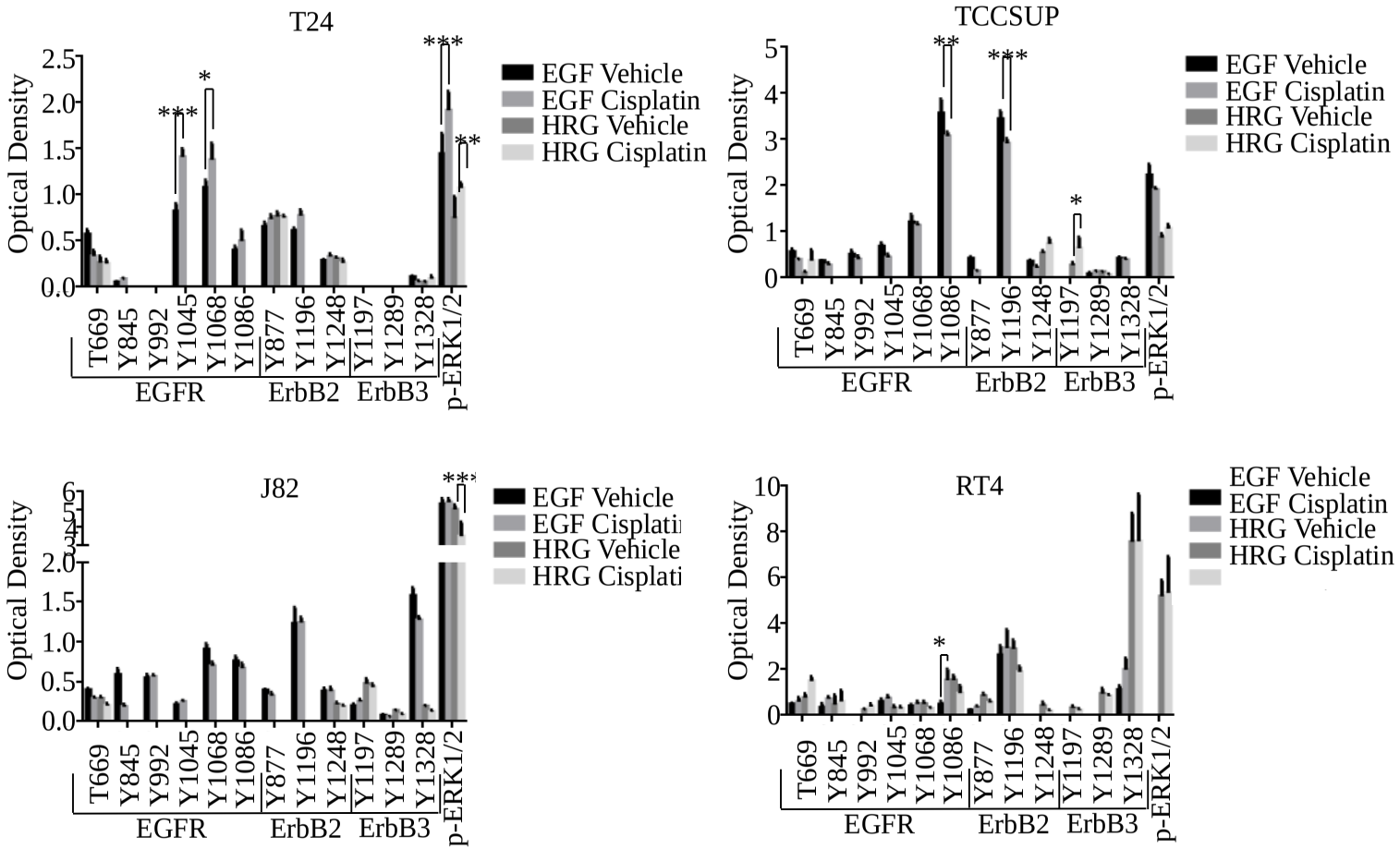

Figure 16. Activation of the EGFR family members following cisplatin treatment. Graphs showing the relative optical density (OD) of each phosphorylation site for each EGFR family member and cell line as determined by ImageJ. Statistical analysis was performed using GraphPad and sites with significantly increased or decreased phosphorylation are indicated. The bars within each graph represent an average of the results obtained from three independent experiments. * = p-value < 0.05 ** = p-value < 0.01 *** = p-value < 0.001. T = threonine, Y = tyrosine.

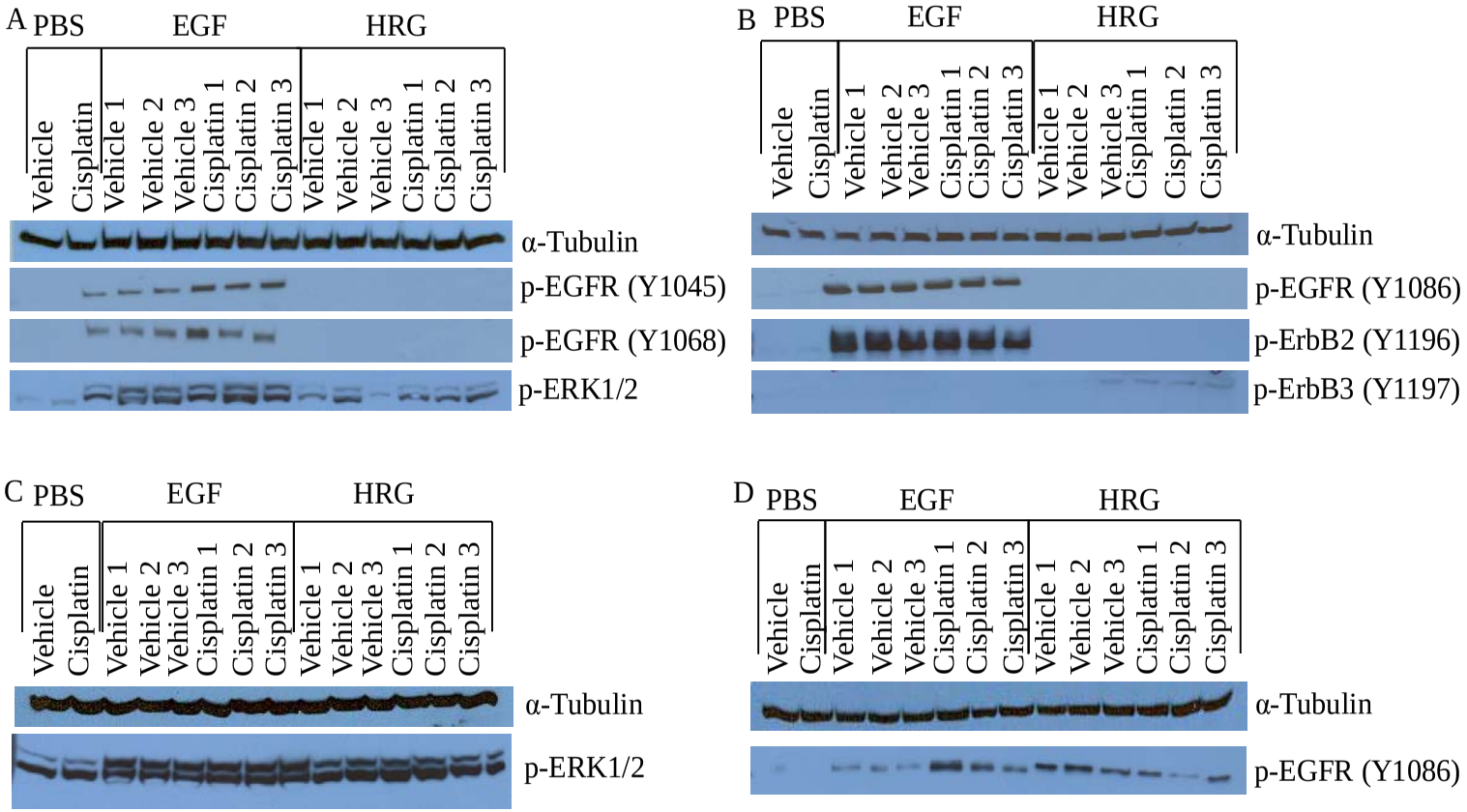

Figure 17. Western blots demonstrating activation of the EGFR family following cisplatin treatment. Western blots showing statistically up- or down-regulated phosphorylation sites of EGFR family members after treatment with cisplatin. Lysates were treated and stimulated as indicated. Blots were probed with antibodies specific to the indicated phosphorylation site. Blots correspond to the cell lines T24 (A), TCCSUP (B), J82 (C), and RT4 (D).

Dose Determination of Pharmacologic Treatments

Given the previously described results and the various reports on the outcomes of clinical trials using ErbB inhibitors (Zachos, Konstantinopoulos et al. 2010, Mooso, Vinall et al. 2014), the question as to whether therapies utilizing ErbB inhibitors could be optimized alone or in combination with standard-of-care was one that seemed wholly applicable to this study. To answer this question, the four bladder cancer cell lines were analyzed for growth retardation by MTT assay using varying concentrations of each of the ErbB inhibitors. This assay was used to determine the optimal doses of trastuzumab, tarceva, lapatinib, and dacomitinib that should be utilized for further experiments. Dose response curves were plotted using GraphPad software (Figure 18), which also determined the IC_{50} for each of the drugs (Table 5). Dacomitinib, the pan-ErbB inhibitor, had the lowest IC_{50} overall followed closely by tarceva and lapatinib (Table 5B-D). The IC_{50} for trastuzumab was too high in the J82 and RT4 cell lines to be considered physiologically relevant, and was determined to be infinite in the TCCSUP cell line (Table 5A). Thus, no further experiments were conducted using trastuzumab. From this data it was determined that future experiments would utilize dacomitinib at a concentration of 1 μM, tarceva at a concentration of 2 μM, and lapatinib at a concentration of 5 μM. These doses were chosen based on the experimentally determined IC_{50} values, and physiologically attainable serum levels previously reported in the literature (Takahashi, Boku et al. 2012, Hudachek and Gustafson 2013, Tiseo, Andreoli et al. 2014).

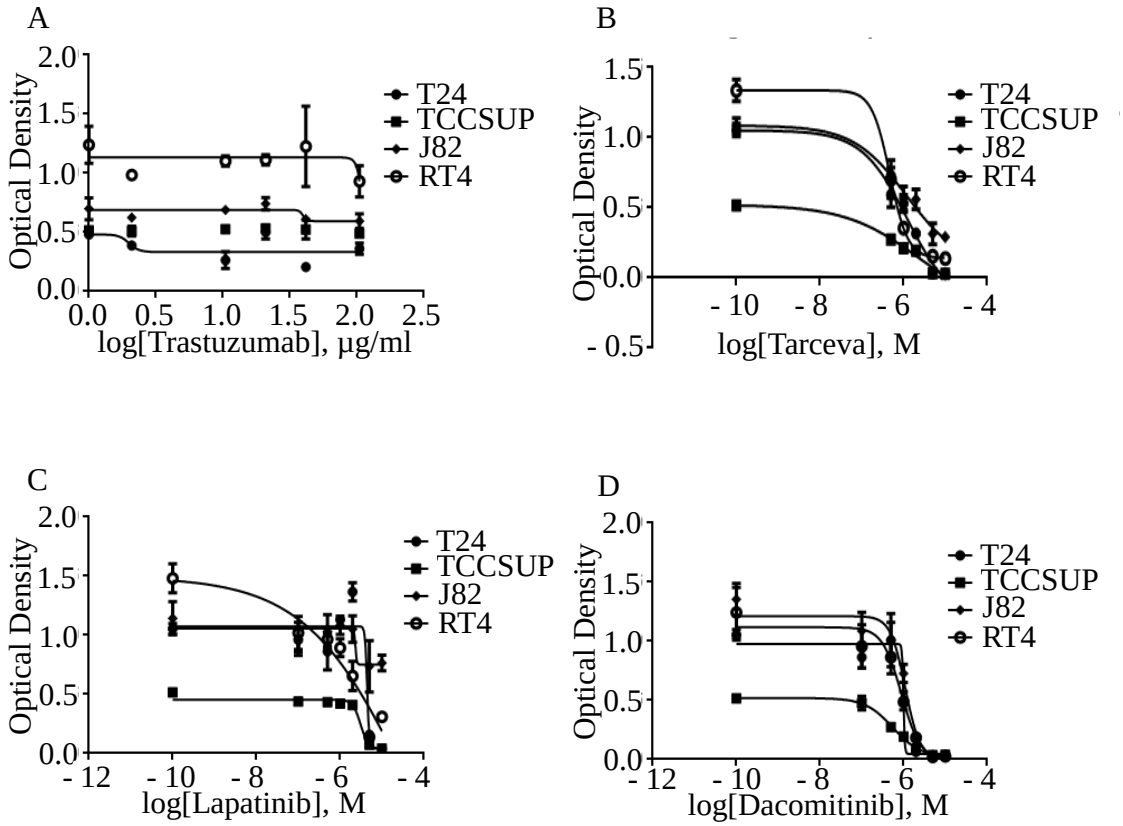

Figure 18. Growth effects of pharmacologic treatments. Graphs show the dose response curves for each cell line when treated with varying concentrations of (A) trastuzumab (B) erlotinib (C) lapatinib or (D) dacomitinib.

Trastuzumab

Cell Line	IC_{50} (95% CI)
T24	1.99 µg/ml (∞)‡
TCCSUP	Not Converged
J82	39.66 µg/ml (∞)
RT4	163.9 µg/ml (∞)

Erlotinib

Cell Line	IC_{50} (95% CI)
T24	1.25 µM (0.50 – 3.1) ‡
TCCSUP	2.21 µM (0.07 – 70.4)
J82	1.18 µM (0.19 – 7.15)
RT4	0.47 µM (0.40 – 0.56)

Lapatinib

Cell Line	IC_{50} (95% CI)
T24	4.45 µM (∞) ‡
TCCSUP	3.09 µM (2.46 – 3.87)
J82	2.33 µM (∞)
RT4	40.2 µM (0.03 pM – 48.7 kM)

Dacomitinib

Cell Line	IC_{50} (95% CI)
T24	0.99 µM (∞) ‡
TCCSUP	0.56 µM (0.46 – 0.67)
J82	1.11 µM (0.89 – 1.38)
RT4	0.89 µM (0.65 – 1.22)

Table 5. IC_{50} determination of pharmacologic treatments. Tables show the computed IC_{50} for pharmacologic agents in each cell line as noted. ‡95% confidence interval.

Effects of Pharmacologic Treatments on Bladder Cancer Cells

In order to determine the appropriate drug concentrations to use in further studies, tarceva, lapatinib, dacomitinib, and cisplatin were used alone or in various combinations in all cell lines. MTT assays were performed to measure effects on growth over five days. Flow cytometry was performed after 72 hours of treatment to measure levels of apoptosis and cell cycle progression. Meanwhile, Western blotting was employed to determine if previously observed alterations in the EGFR family signaling pathway were also induced by any of the investigated therapeutics.

Western blot analysis of the T24 and J82 cell lines revealed that only when T24 cells were stimulated with EGF were they susceptible to inhibition of ERK1/2 phosphorylation by the ErbB inhibitors (Figure 19A, D). This was determined by the observed decrease in band intensity. In contrast, when T24 or J82 cells were stimulated with HRG, ERK1/2 phosphorylation was unchanged by treatment with the ErbB inhibitors (Figure 19B, C).

MTT assays determined that no one combination was the most effective therapeutic in every cell line (Figure 20). This is in spite of the observation that all cell lines had their growth inhibited by the various combinations of drugs tested. The determination of “most effective combination” was made by determining which of the combinations of drugs induced the greatest growth inhibition, while at the same time minimizing the number of drugs used. This was done so as to reduce side effects and toxicity as these could render any proposed combinations unusable in a clinical setting.

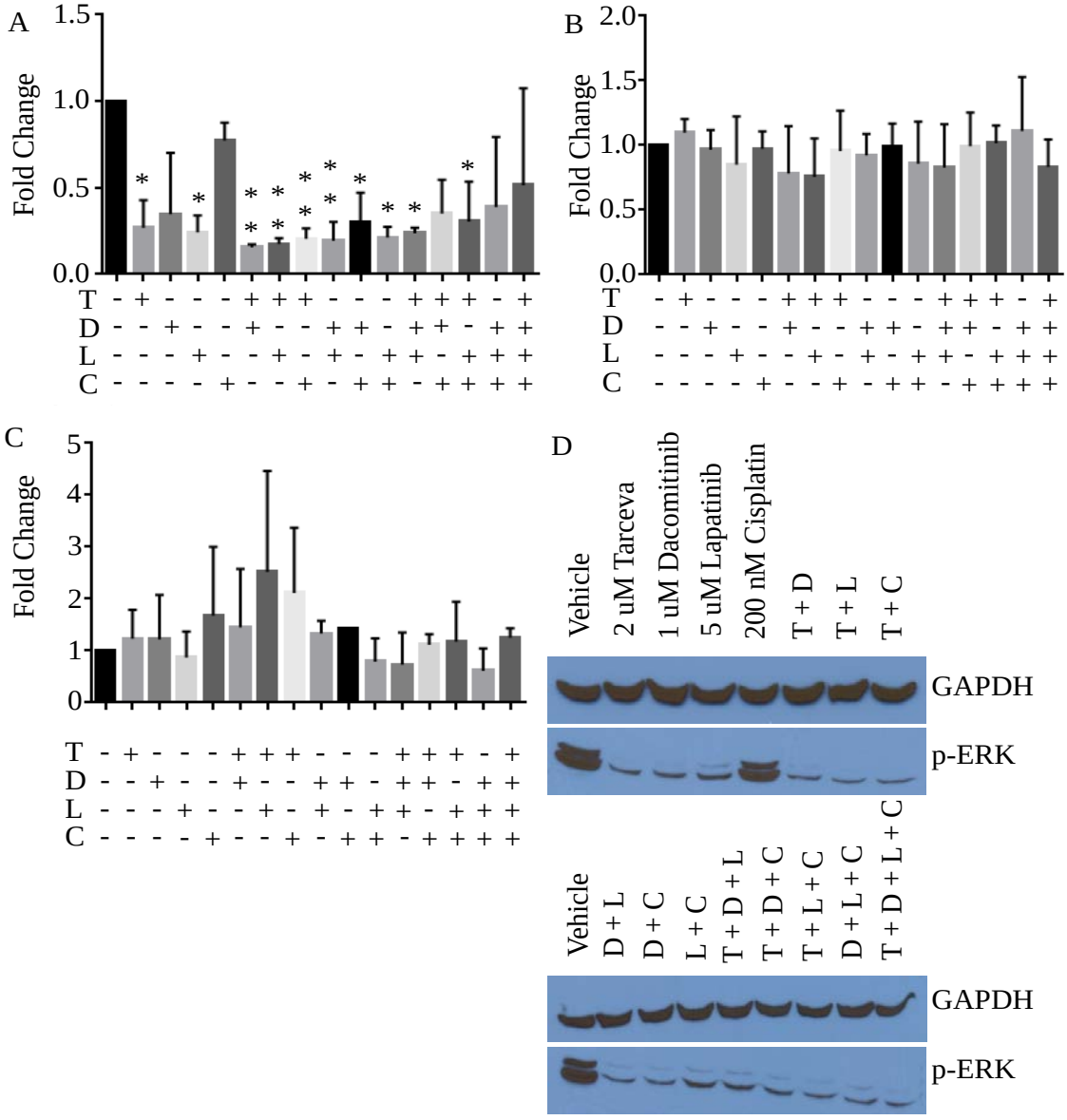

Figure 19. Effect of ErbB inhibitors and cisplatin on downstream ErbB targets. (A-C) Each bar depicts the average optical density of three independent western blotting experiments normalized to the vehicle control of each individual experiment. Significance indicators show the comparison with the treatment indicated and the vehicle control. (A) T24 cells stimulated with EGF. (B) T24 cells stimulated with HRG. (C) J82 cells stimulated with HRG. (D) Representative western blots of T24 cells treated as indicated and stimulated with EGF. * = p-value < 0.05 ** = p-value < 0.01. T = 2 μM tarceva, D = 1 μM dacomitinib, L = 5 μM lapatinib, C = 200 nM cisplatin

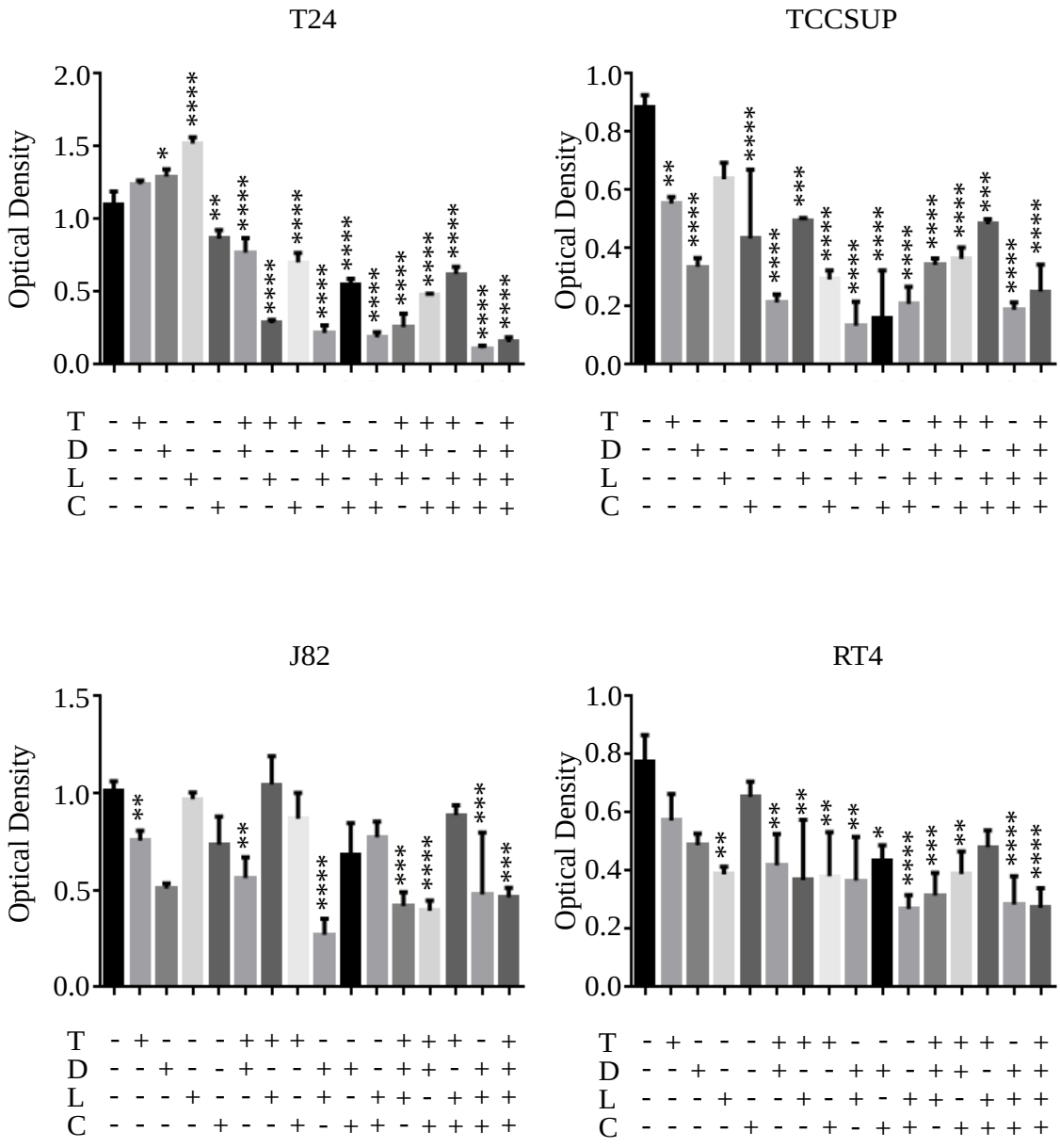

Figure 20. Growth effects due to pharmacologic therapies. Graphs depicting the day 5 results of MTT assays conducted on each cell line. The bars within each graph represent an average of the results obtained from three independent experiments. Significance indicators represent the difference between the indicated treatment and vehicle. * = p-value < 0.05, ** = p-value < 0.01, *** = p-value < 0.001, **** = p-value < 0.0001. T = 2 µM tarceva, D = 1 µM dacomitinib, L = 5 µM lapatinib, C = 200 nM cisplatin

The combination of lapatinib and cisplatin was determined to be most effective in T24 cells (Figure 20A). Meanwhile, dacomitinib alone was determined to be the most effective treatment in TCCSUP cells (Figure 20B). Similarly, the combination of dacomitinib and lapatinib was determined to be most effective in J82 cells (Figure 20C). Finally, lapatinib alone was determined to be most effective in RT4 cells (Figure 20D). In all cases, growth inhibition using what was determined to be the "most effective combination" for each cell line was observed to be between 50% and 75% of vehicle treated cells (Figure 20).

Flow cytometric assays were employed to determine if these various drugs, alone or in combination, had any effect on the cell cycle (Figure 21), or the rate of apoptosis (Figure 22) in these cells. Amount of apoptosis is determined by the amount of cells in the lower right-hand quadrant of a flow cytometry density plot. Plots are generated such that Annexin-V is plotted on the X-axis and propidium iodide is plotted on the Y-axis. In both cases, the only statistically significant effect that was observed was an increase in the amount of TCCSUP cells in G2 when treated with the combination of tarceva and cisplatin (Figure 21).

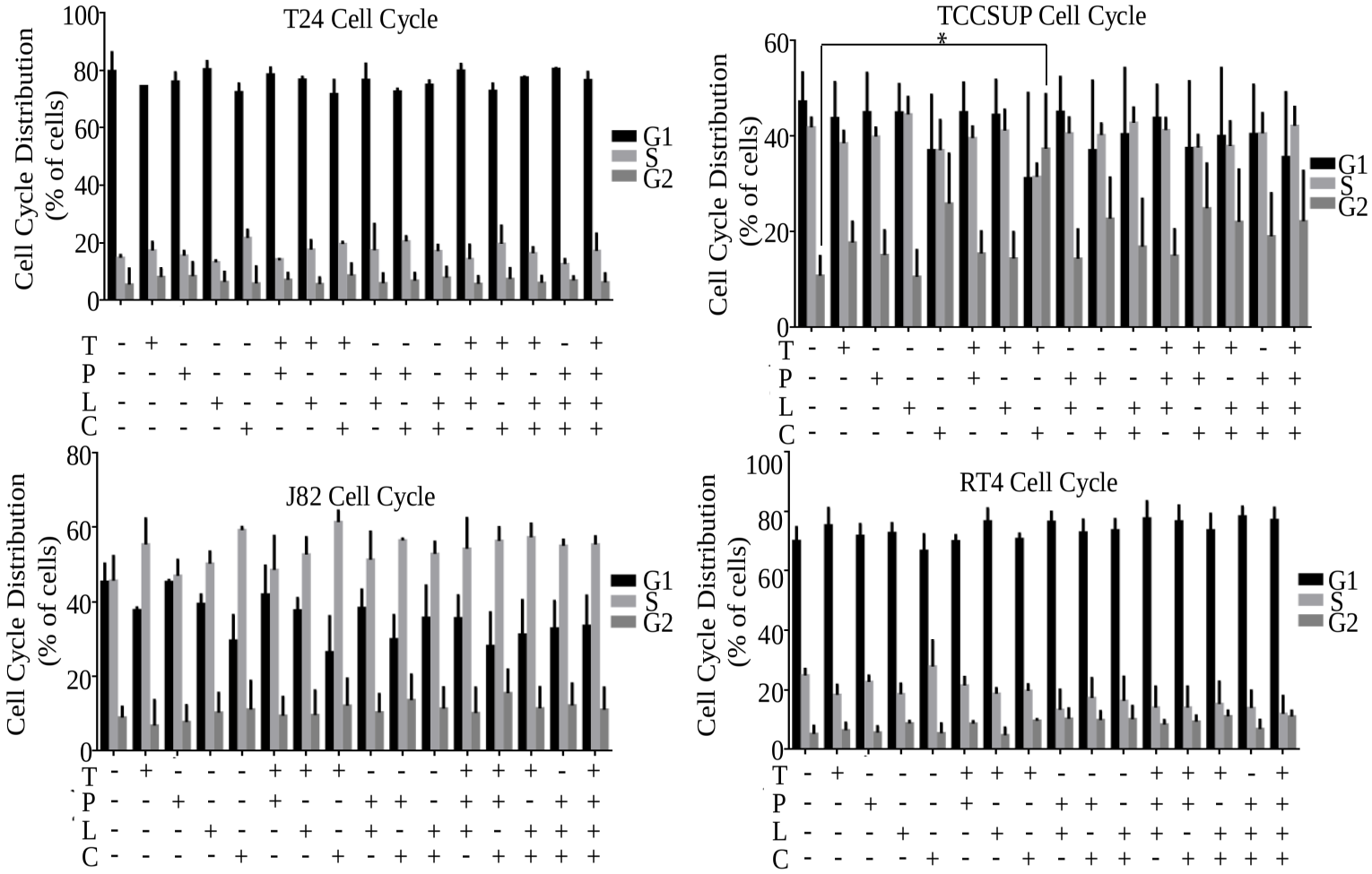

Figure 21. Effect of pharmacologic therapies on cell cycle progression. Graphs showing the relative amount of cell in each phase of the cell cycle when treated with various pharmacologic treatments. Each bar represents the mean of the results obtained from three, or four in the case of the TCCSUP cell line, independent experiments ± standard deviation. * = p-value < 0.05. T = 2 µM tarceva, P = 1 µM PF00299804 (dacomitinib), L = 5 µM lapatinib, C = 200 nM cisplatin

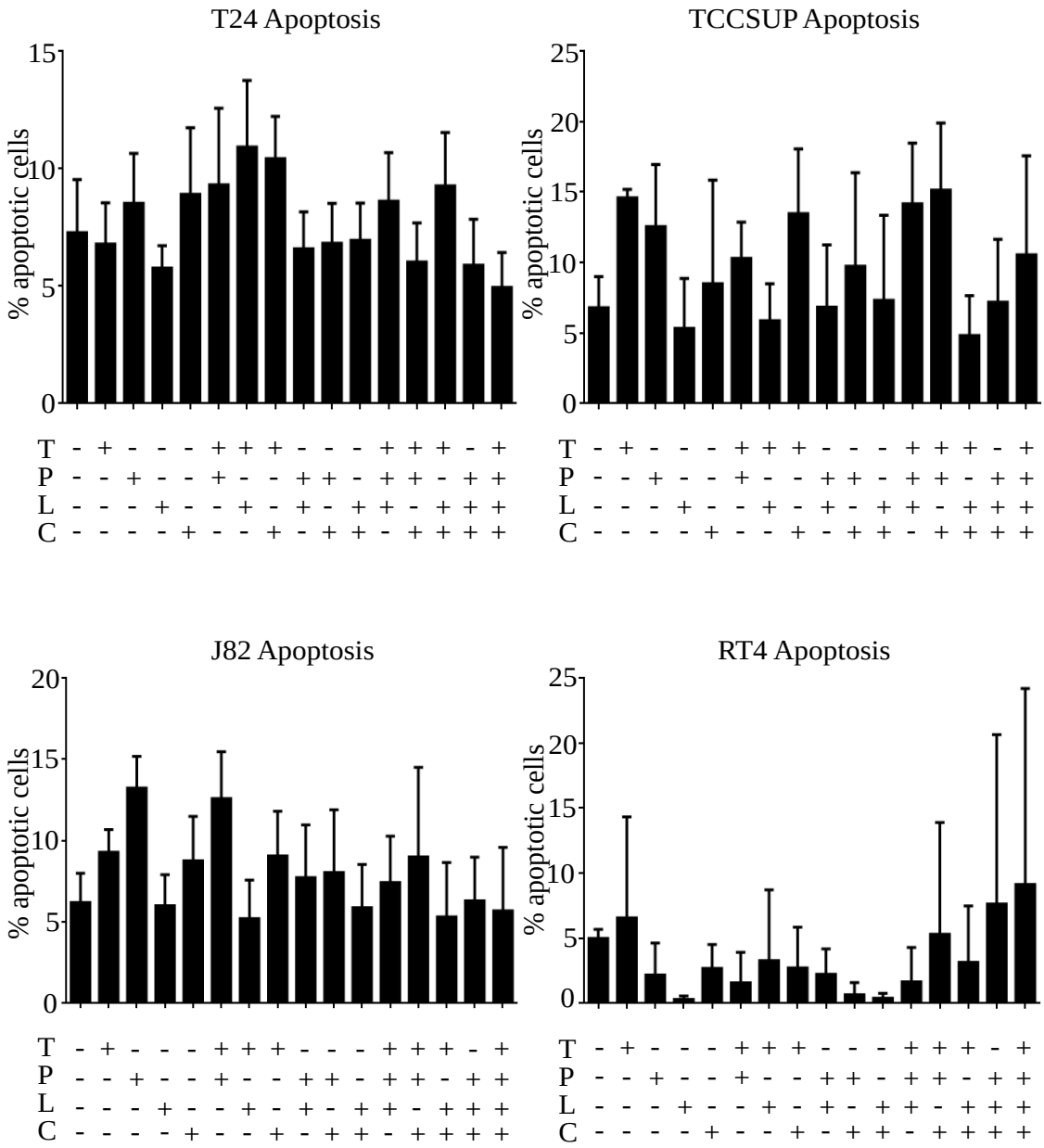

Figure 22. The effect of pharmacologic therapies on apoptosis of bladder cancer cells. Graphs showing the relative amount of apoptosis in each cell line with various pharmacologic treatments. Each bar represents the mean of the results obtained from three, or four in the case of the TCCSUP cell line, independent experiments ± standard deviation. T = 2 μM tarceva, P = 1 μM PF00299804 (dacomitinib), L = 5 μM lapatinib, C = 200 nM cisplatin

DISCUSSION

De novo and acquired resistance to cisplatin remains a major hindrance to developing effective treatments for patients with advanced bladder cancer. Much of the literature suggests that answers to overcoming this resistance may be found in the recently developed ErbB inhibitors. With overexpression of the EGFR family prevalent in bladder cancer cell lines and tissues (Chow, Liu et al. 1997, Chow, Chan et al. 2001), there has been a recent abundance of clinical trials utilizing ErbB inhibitors in the neoadjuvant, adjuvant, or second-line setting. These trials have sought to determine if these inhibitors could improve on the current standard-of-care (Zachos, Konstantinopoulos et al. 2010, Mooso, Vinall et al. 2014). Unfortunately, no previous trials have been successful in determining a therapeutic regimen which provides additional benefit when compared to standard-of-care. It is for this reason that the current study was conducted. It was widely evident (Mooso, Vinall et al. 2014) that more basic research needed to be done to determine a mechanism for resistance towards cisplatin and ErbB inhibitors.

The initial results, looking at cell growth in response to knockdown of the EGFR and ErbB2 proteins, were encouraging. They were encouraging in that cellular growth seemed to be inhibited by protein knockdown (Figures 4 & 6). While the results of the MTT assays revealed that cellular growth was slowed by the knockdown of these proteins, there was no significant increase in apoptosis in the majority of cell lines (Figure 7). Additionally, there was no apparent arrest of the cisplatin-resistant cell lines

T24, TCCSUP, and RT4 in any of the phases of the cell cycle (Figure 8 and 9). This indicated that cells had their growth rates slowed rather than undergoing apoptotic cell death or growth arrest, as either of these changes would have been observed in the flow cytometry assays. In addition, treatment with cisplatin was able to reverse the increase in apoptosis and cell cycle arrest produced by treatment with ErbB2 siRNA in the T24 cell line (Figure 7). Since the entirety of the cell lines used in this study were derived from patients who had not previously received chemotherapy, those cell lines which are resistant to treatment with cisplatin represent intrinsic cisplatin resistance. Thus, these results indicate that standard-of-care treatment may actually be detrimental to patients with *de novo* cisplatin resistance. This is due to standard-of-care currently consisting of treatment with cisplatin. According to these results, standard-of-care would not only have no effect, but would also render the cells resistant to therapies which target ErbB2. With this in mind then, the results from this study clearly indicate that clinical care for patients with MIBC should take *de novo* cisplatin-resistance into account, and should screen for resistance using the excised tissue obtained from the patient's radical cystectomy.

Furthermore, the observed inability of ErbB3 siRNA to knockdown the ErbB3 protein in cisplatin-resistant cells (Figure 10) raises another serious question. This inability to knock-down ErbB3 protein levels suggests that dysregulation of protein degradation pathways may be a part of the oncogenic transformation of bladder epithelial cells. If this is indeed the case, this process would then confer resistance to

ErbB inhibitors by creating a stabilized ErbB3 protein. Stabilized ErbB3 would then be free to propagate signaling through the PI3K pathway by forming heterodimers with ErbB4, as most clinical ErbB inhibitors do not inhibit ErbB4.

In order for a protein to be degraded in a mammalian cell, the protein must first be marked for degradation. In the case of ErbB3, it must be marked by the addition of ubiquitin molecules, commonly added by a protein called Nrdp1 (Cao, Wu et al. 2007). This then allows for the protein to be degraded by the proteasome. Thus, disruption of ubiquitin ligases such as Nrdp1 may have a cascading effect leading to increased ErbB3 stability. Additionally, the ErbB3-binding protein EBP1 is present both in the cytoplasm and nucleus, but is only active in the nucleus. EBP1 has been shown to be mediated by ErbB3 activation (Yoo, Wang et al. 2000), as EBP1 binds to ErbB3 only when ErbB3 is in a dephosphorylated state. This binding sequesters EBP1 in the cytoplasm, and prevents EBP1 from having its traditional inhibitory effect on cell proliferation (Hu, Xiong et al. 2014). Furthermore, ectopic expression of EBP1 in a breast cancer cell line was able to reduce cell proliferation, and formation of colonies (Lessor, Yoo et al. 2000). Thus, increased PI3K signaling along with disruption of the EBP1 pathway could lead to increased cellular survival and proliferation.

Significantly, ErbB3 signaling has been shown to confer resistance to ErbB inhibitors in other cancer models (Hu, Venkateswarlu et al. 2005, Ono and Kuwano 2006, Engelman, Zejnullahu et al. 2007, Chen, Mooso et al. 2011, Vaught, Stanford et al. 2012). This finding is even more devastating in light of the observation that

successful knockdown of the ErbB3 protein in the J82 cell line caused many important observations. ErbB3 knockdown caused a nearly 100% growth inhibition (Figure 13), a statistically significant G1 arrest (Figure 14), and a more than two-fold increase in the level of apoptosis (Figure 15). This demonstrates that ErbB3 is a highly relevant target in advanced bladder cancer. Of note, treatment with ErbB3 siRNA and cisplatin abrogated the G1 arrest seen with ErbB3 siRNA treatment alone. Similar to the effect that addition of cisplatin to ErbB2 siRNA treatment had on apoptosis in the T24 cell line, addition of cisplatin also induced a concomitant G2 arrest (Figure 14). This is a promising factor as a G2 arrest would indicate that, instead of merely slowing down the cellular growth, the cells would be likely to apoptose. This increase in apoptosis could then provide a durable cure for TCC. Unfortunately, a significant increase in apoptosis was not observed in the J82 cell line in this study.

The effects of cisplatin on the EGFR family and downstream target activation were next explored. No universal pattern was readily apparent amongst the cell lines studied; however, there was a tendency for the cisplatin-resistant cell lines to have levels of phosphorylated ERK1/2 increased by treatment with cisplatin and stimulation with HRG (Figure 16). Sadly, this trend only reached the level of statistical significance in the case of T24 cells. This observation is in agreement with the earlier findings of the MTT and flow cytometer assays. This determination was made because increased levels of ERK1/2 phosphorylation would lead to increased cell growth and

survival, as previously reported in the literature (Kyriakis, App et al. 1992, Leevers and Marshall 1992).

Bladder cancer cells were next treated with various pharmacologic therapies to see if ligand-induced ErbB activation could be abrogated. When determining appropriate treatment concentrations for each of the drugs, it was surprising that trastuzumab was not more effective at inhibiting cellular growth. This observation was surprising as the previous observations utilizing the ErbB2 siRNA were quite promising in the TCCSUP cell line (Figure 8). However, trastuzumab only affects cells which overexpress ErbB2 through an *ERBB2* amplification, increased protein stability, or increased protein production, none of which were observed in these cells (Figure 2).

Notably, when T24 cells were treated with the various ErbB inhibitors and stimulated with EGF, the downstream signaling was almost universally downregulated as determined by a statistical drop in optical density (Figure 19A). The notable exception to this was when cisplatin was used as a monotherapy; however, addition of any inhibitor to the cisplatin regimen was able to induce a downregulation of ERK phosphorylation. In contrast, when either the T24 or J82 cell lines were treated with these drugs and stimulated with HRG no statistically significant effect on ERK1/2 phosphorylation was observed. This further demonstrates the importance of ErbB3 signaling in the propagation of advanced bladder cancer (Figure 19B, C). Again, this would suggest that in patients with *de novo* cisplatin resistance the standard-of-care treatment may actually do more harm than good. This observation indicates that

cisplatin seems to activate this survival pathway, and cause cellular proliferation to continue unchecked. The current literature points to glutathione as a mediator of this process.

Several reports have indicated that cells which are cisplatin-resistant produce higher levels of glutathione than their cisplatin-sensitive counterparts (Balendiran, Dabur et al. 2004, Stordal and Davey 2007). In contrast to the earlier observations, it has also been shown that increased levels of glutathione in cells serve to decrease ERK activation (Lu and Cederbaum 2007). Study of urologic tissue in response to cisplatin has shown that when cisplatin is administered, reduced-glutathione concentrations are increased while oxidized-glutathione, also known as L-(-)-glutathione, levels remain unchanged (Mistry, Merazga et al. 1991). This evidence indicates that while there is plenty of glutathione available, it does not perform its intended function of inactivating reactive oxygen species (ROS), as reduced-glutathione is the pre-reaction form. Therefore, if glutathione were performing as it should, there should also be a concomitant increase in oxidized-glutathione levels as levels of ROS are generally elevated in cancerous cells (Cerutti 1985, Wu 2006). Therefore, it may be possible that the T24 bladder cancer cell line is increasing glutathione production in response to treatment with cisplatin. Meanwhile, the cisplatin is preventing the glutathione from having its traditional inhibitory effect on ERK phosphorylation. Together this would cause a concomitant increase in ERK activation.

Finally, cells were assayed for growth (Figure 20), cell cycle progression (Figure 21), and survival (Figure 22). Through these assays it became apparent that while many of the treatments would serve to inhibit cell growth, no treatment regimen was effective in all three areas of investigation. In fact, only the TCCSUP cell line experienced any significant cell cycle arrests, and no cell lines were observed to have a significant increase in apoptosis.

In part, this would seem to be attributable to the variable way in which these cells respond to stimulus. For example, the T24 and RT4 cell lines primarily phosphorylated EGFR and ErbB2 upon stimulation with EGF (Figure 16). Since these proteins were the primary EGFR family members activated, these cell lines must primarily use these proteins for survival when growth stimulus is present. The observation that these cell lines respond best to treatment with lapatinib, an EGFR/ErbB2 dual-kinase inhibitor, as opposed to other ErbB inhibitors is not surprising. Similarly, the J82 and TCCSUP cell lines respond primarily to treatment with dacomitinib, a pan-ErbB inhibitor. Since they activate EGFR, ErbB2, and ErbB3 in response to stimulation with EGF (Figure 16), this comes as no surprise.

Taken together, the clinical implication of the results in Figures 20, 21, and 22 is that addition of these ErbB inhibitors to standard-of-care should increase patient survival. However, it should not be expected that ErbB inhibitors would provide a durable cure for this disease. This is because the ErbB inhibitors do not increase apoptosis or cell cycle arrest in these cell lines. However, this is not what has been

observed in several clinical trials which have utilized these therapies (Zachos, Konstantinopoulos et al. 2010, Mooso, Vinall et al. 2014). This dichotomy of findings between previous clinical trials and the data described herein clearly point to the need for a better and more complete understanding of the molecular mechanisms underlying both bladder cancer development and cisplatin resistance.

While that research is being conducted, there are measures that can be incorporated into the current standard-of-care to better serve patients. The first of these measures is a more personalized approach toward determining a patient's chemotherapeutic regimen. It is clear that there are at least two distinct subsets of patients: one comprised of those patients who have cisplatin-sensitive bladder cancer, and the other comprised of patients with cisplatin-resistant bladder cancer. Since current standard-of-care would be effective for cisplatin-sensitive patients, they would be given standard-of-care. Meanwhile, cisplatin-resistant patients would be given an alternate treatment. This is important as it has already been demonstrated how cisplatin treatment of cisplatin-resistant cells can lead to further resistance toward other therapies.

The determination of which patients were sensitive or resistant to cisplatin would require the development of a biomarker. As has been already observed in the literature (Balendiran, Dabur et al. 2004, Stordal and Davey 2007), glutathione levels are significantly increased in tumors which are cisplatin-resistant. Therefore, a glutathione staining of the resected tissue, when compared to normal bladder tissue

from the same patient, could serve to determine which patients are cisplatin-resistant. The query then changes to determining the best course of treatment for these individuals. Previous studies with the ERK inhibitor U0126 and L-buthionine sulfoximine have shown that combining these compounds with cisplatin treatment is effective. This treatment re-sensitizes cancerous cells to cisplatin therapy. Importantly, these re-sensitized cells have been observed to undergo apoptotic cell death in response to this treatment as opposed to necrotic cell death (Lu and Cederbaum 2007). This observation is important as necrotic cell death could prove to be highly toxic for the patient and could lead to patient death.

CONCLUSIONS

An understanding of the expression profile of the EGFR family in advanced bladder cancer has been in the forefront of the research community for the last couple of decades. Unfortunately, not much work has been done to elucidate the importance and interconnected relations this family plays in the larger treatment landscape. This current study demonstrates that current standard-of-care may be harmful to patients with *de novo* resistance to cisplatin. Additionally, this study demonstrates that downstream EGFR family signaling plays an important role in the survival of advanced bladder cancer. Going forward, the role of glutathione as a biomarker for the determination of cisplatin-resistance should be explored. Additionally, the combination of the ERK inhibitor U0126, L-buthionine sulfoximine, and cisplatin should be explored. It is possible that this will provide a valuable chemotherapeutic regimen for patients with cisplatin-resistant bladder cancer. These additions to standard-of-care practices could vastly improve the outcomes for patients with MIBC by leading to increased survival times and reducing the risk of recurrence.

LITERATURE CITED

Amsellem-Ouazana, D., I. Bièche, S. Tozlu, H. Botto, B. Debré and R. Lidereau (2006). "Gene expression profiling of ERBB receptors and ligands in human transitional cell carcinoma of the bladder." The Journal of Urology **175**(3): 1127-1132.

Apolo, A. B., B. Bochner, S. M. Steinberg, D. F. Bajorin, W. K. Kelly, D. I. Quinn, N. J. Vogelzang and S. S. Sridhar (2012). "Examining the management of muscle-invasive bladder cancer (MIBC) by medical oncologists (MO)." J Clin Oncol **30**(5_suppl): 298.

Balendiran, G. K., R. Dabur and D. Fraser (2004). "The role of glutathione in cancer." Cell Biochem Funct **22**(6): 343-352.

Baliga, B. S., A. W. Pronczuk and H. N. Munro (1969). "Mechanism of cycloheximide inhibition of protein synthesis in a cell-free system prepared from rat liver." J Biol Chem **244**(16): 4480-4489.

Bieche, I., P. Onody, S. Tozlu, K. Driouch, M. Vidaud and R. Lidereau (2003). "Prognostic value of ERBB family mRNA expression in breast carcinomas." Int J Cancer **106**(5): 758-765.

Bindels, E. M., T. H. van der Kwast, V. Izadifar, D. K. Chopin and W. I. de Boer (2002). "Functions of epidermal growth factor-like growth factors during human urothelial reepithelialization in vitro and the role of erbB2." Urol Res **30**(4): 240-247.

Brincks, E. L., M. C. Risk and T. S. Griffith (2013). "PMN and anti-tumor immunity--the case of bladder cancer immunotherapy." Semin Cancer Biol **23**(3): 183-189.

Bubenik, J., M. Baresova, V. Viklicky, J. Jakoubkova, H. Sainerova and J. Donner (1973). "Established cell line of urinary bladder carcinoma (T24) containing tumour-specific antigen." Int J Cancer **11**(3): 765-773.

Cao, Z., X. Wu, L. Yen, C. Sweeney and K. L. Carraway, 3rd (2007). "Neuregulin-induced ErbB3 downregulation is mediated by a protein stability cascade involving the E3 ubiquitin ligase Nrdp1." Mol Cell Biol **27**(6): 2180-2188.

Cerutti, P. A. (1985). "Prooxidant states and tumor promotion." Science **227**(4685): 375-381.

Chaux, A., J. S. Cohen, L. Schultz, R. Albadine, S. Jadallah, K. M. Murphy, R. Sharma, M. P. Schoenberg and G. J. Netto (2012). "High epidermal growth factor receptor immunohistochemical expression in urothelial carcinoma of the bladder is not associated with EGFR mutations in exons 19 and 21: a study using formalin-fixed, paraffin-embedded archival tissues." Hum Pathol **43**(10): 1590-1595.

Chen, L., B. A. Mooso, M. K. Jathal, A. Madhav, S. D. Johnson, E. van Spyk, M. Mikhailova, A. Zierenberg-Ripoll, L. Xue, R. L. Vinall, R. W. deVere White and P. M. Ghosh (2011). "Dual EGFR/HER2 inhibition sensitizes prostate cancer cells to androgen withdrawal by suppressing ErbB3." Clin Cancer Res **17**(19): 6218-6228.

Chow, N. H., S. H. Chan, T. S. Tzai, C. L. Ho and H. S. Liu (2001). "Expression profiles of ErbB family receptors and prognosis in primary transitional cell carcinoma of the urinary bladder." Clin Cancer Res **7**(7): 1957-1962.

Chow, N. H., H. S. Liu, H. B. Yang, S. H. Chan and I. J. Su (1997). "Expression patterns of erbB receptor family in normal urothelium and transitional cell carcinoma. An immunohistochemical study." Virchows Arch **430**(6): 461-466.

Engelman, J. A., K. Zejnullahu, C. M. Gale, E. Lifshits, A. J. Gonzales, T. Shimamura, F. Zhao, P. W. Vincent, G. N. Naumov, J. E. Bradner, I. W. Althaus, L. Gandhi, G. I. Shapiro, J. M. Nelson, J. V. Heymach, M. Meyerson, K. K. Wong and P. A. Janne (2007). "PF00299804, an irreversible pan-ERBB inhibitor, is effective in lung cancer models with EGFR and ERBB2 mutations that are resistant to gefitinib." Cancer Res **67**(24): 11924-11932.

Engelman, J. A., K. Zejnullahu, T. Mitsudomi, Y. Song, C. Hyland, J. O. Park, N. Lindeman, C. M. Gale, X. Zhao, J. Christensen, T. Kosaka, A. J. Holmes, A. M. Rogers, F. Cappuzzo, T. Mok, C. Lee, B. E. Johnson, L. C. Cantley and P. A. Janne (2007). "MET amplification leads to gefitinib resistance in lung cancer by activating ERBB3 signaling." Science **316**(5827): 1039-1043.

Guancial, E. A., J. E. Rosenberg and C. J. Sweeney (2011). Update in urothelial carcinoma: Novel agents and targeted therapy. ASCO: Genitourinary Cancer Education Book 2011**:** 171 - 176.

Gunes, S., Y. Sullu, Z. Yegin, R. Buyukalpelli, L. Tomak and H. Bagci (2013). "ErbB receptor tyrosine kinase family expression levels in urothelial bladder carcinoma." Pathol Res Pract **209**(2): 99-104.

Hu, B., Y. Xiong, R. Ni, L. Wei, D. Jiang, G. Wang, D. Wu, T. Xu, F. Zhao, M. Zhu and C. Wan (2014). "The downregulation of ErbB3 binding protein 1 (EBP1) is associated with poor prognosis and enhanced cell proliferation in hepatocellular carcinoma." Mol Cell Biochem **396**(1-2): 175-185.

Hu, Y. P., S. Venkateswarlu, N. Sergina, G. Howell, P. St Clair, L. E. Humphrey, W. Li, J. Hauser, E. Zborowska, J. K. Willson and M. G. Brattain (2005). "Reorganization of ErbB family and cell survival signaling after Knock-down of ErbB2 in colon cancer cells." J Biol Chem **280**(29): 27383-27392.

Hubbard, S. R. and J. H. Till (2000). "Protein tyrosine kinase structure and function." Annu Rev Biochem **69**: 373-398.

Hudachek, S. F. and D. L. Gustafson (2013). "Physiologically based pharmacokinetic model of lapatinib developed in mice and scaled to humans." J Pharmacokinet Pharmacodyn **40**(2): 157-176.

Jathal, M. K., L. Chen, M. Mudryj and P. M. Ghosh (2011). "Targeting ErbB3: the new RTK(id) on the prostate cancer block." Immunol Endocr Metab Agents Med Chem **11**(2): 131-149.

Junttila, T. T., M. Laato, T. Vahlberg, K. O. Soderstrom, T. Visakorpi, J. Isola and K. Elenius (2003). "Identification of patients with transitional cell carcinoma of the bladder overexpressing ErbB2, ErbB3, or specific ErbB4 isoforms: real-time reverse transcription-PCR analysis in estimation of ErbB receptor status from cancer patients." Clin Cancer Res **9**(14): 5346-5357.

Koopman, G., C. P. Reutelingsperger, G. A. Kuijten, R. M. Keehnen, S. T. Pals and M. H. van Oers (1994). "Annexin V for flow cytometric detection of phosphotidylserine expression on B cells undergoing apoptosis." Blood **84**(5): 1415-1420.

Kyriakis, J. M., H. App, X. F. Zhang, P. Banerjee, D. L. Brautigan, U. R. Rapp and J. Avruch (1992). "Raf-1 activates MAP kinase-kinase." Nature **358**(6385): 417-421.

Larsen, W. J. (2001). Human Embryology.

Lazzeri, M. (2006). "The physiological function of the urothelium--more than a simple barrier." Urol Int **76**(4): 289-295.

Leevers, S. J. and C. J. Marshall (1992). "Activation of extracellular signal-regulated kinase, ERK2, by p21ras oncoprotein." EMBO J **11**(2): 569-574.

Lessor, T. J., J.-Y. Yoo, X. Xia, N. Woodford and A. W. Hamburger (2000). "Ectopic expression of the ErbB-3 binding protein Ebp1 inhibits growth and induces differentiation of human breast cancer cell lines." Journal of Cellular Physiology **183**(3): 321-329.

Lu, Y. and A. Cederbaum (2007). "The mode of cisplatin-induced cell death in CYP2E1-overexpressing HepG2 cells: modulation by ERK, ROS, glutathione, and thioredoxin." Free Radic Biol Med **43**(7): 1061-1075.

Messing, E., J. R. Gee, D. R. Saltzstein, K. Kim, A. diSant'Agnese, J. Kolesar, L. Harris, A. Faerber, T. Havighurst, J. M. Young, M. Efros, R. H. Getzenberg, M. A. Wheeler, J. Tangrea, H. Parnes, M. House, J. E. Busby, R. Hohl and H. Bailey (2012). "A phase 2 cancer chemoprevention biomarker trial of isoflavone G-2535 (genistein) in presurgical bladder cancer patients." Cancer Prev Res (Phila) **5**(4): 621-630.

Mistry, P., Y. Merazga, D. J. Spargo, P. A. Riley and D. C. McBrien (1991). "The effects of cisplatin on the concentration of protein thiols and glutathione in the rat kidney." Cancer Chemother Pharmacol **28**(4): 277-282.

Moore, A., C. J. Donahue, K. D. Bauer and J. P. Mather (1998). "Simultaneous measurement of cell cycle and apoptotic cell death." Methods Cell Biol **57**: 265-278.

Mooso, B. A., R. L. Vinall, M. Mudryj, S. A. Yap, R. W. deVere White and P. M. Ghosh (2014). "The role of EGFR family inhibitors in muscle-invasive bladder cancer: A review of clinical data and molecular evidence." The Journal of Urology.

Nayak, S. K., C. O'Toole and Z. H. Price (1977). "A cell line from an anaplastic transitional cell carcinoma of human urinary bladder." Br J Cancer **35**(2): 142-151.

Neal, D. E., L. Sharples, K. Smith, J. Fennelly, R. R. Hall and A. L. Harris (1990). "The epidermal growth factor receptor and the prognosis of bladder cancer." Cancer **65**(7): 1619-1625.

O'Reilly, B. A., A. H. Kosaka, T. K. Chang, A. P. Ford, R. Popert and S. B. McMahon (2001). "A quantitative analysis of purinoceptor expression in the bladders of patients with symptomatic outlet obstruction." BJU Int **87**(7): 617-622.

O'Toole, C., Z. H. Price, Y. Ohnuki and B. Unsgaard (1978). "Ultrastructure, karyology and immunology of a cell line originated from a human transitional-cell carcinoma." Br J Cancer **38**(1): 64-76.

Olayioye, M. A., R. M. Neve, H. A. Lane and N. E. Hynes (2000). "The ErbB signaling network: receptor heterodimerization in development and cancer." EMBO J **19**(13): 3159-3167.

Ono, M. and M. Kuwano (2006). "Molecular mechanisms of epidermal growth factor receptor (EGFR) activation and response to gefitinib and other EGFR-targeting drugs." Clin Cancer Res **12**(24): 7242-7251.

Rajkumar, T., G. W. Stamp, H. S. Pandha, J. Waxman and W. J. Gullick (1996). "Expression of the type 1 tyrosine kinase growth factor receptors EGF receptor, c-erbB2 and c-erbB3 in bladder cancer." The Journal of Pathology **179**(4): 381 - 385.

Rigby, C. C. and L. M. Franks (1970). "A human tissue culture cell line from a transitional cell tumour of the urinary bladder: growth, chromosone pattern and ultrastructure." Br J Cancer **24**(4): 746-754.

Rotterud, R., J. M. Nesland, A. Berner and S. D. Fossa (2005). "Expression of the epidermal growth factor receptor family in normal and malignant urothelium." BJU Int **95**(9): 1344-1350.

Royer, B., D. Delroeux, E. Guardiola, M. Combe, G. Hoizey, D. Montange, J. P. Kantelip, B. Chauffert, B. Heyd and X. Pivot (2008). "Improvement in intraperitoneal intraoperative cisplatin exposure based on pharmacokinetic analysis in patients with ovarian cancer." Cancer Chemother Pharmacol **61**(3): 415-421.

Schulze, W. X., L. Deng and M. Mann (2005). "Phosphotyrosine interactome of the ErbB-receptor kinase family." Mol Syst Biol **1**: 2005 0008.

Sergina, N. V., M. Rausch, D. Wang, J. Blair, B. Hann, K. M. Shokat and M. M. Moasser (2007). "Escape from HER-family tyrosine kinase inhibitor therapy by the kinase-inactive HER3." Nature **445**(7126): 437-441.

Soule, H. D., J. Vazguez, A. Long, S. Albert and M. Brennan (1973). "A human cell line from a pleural effusion derived from a breast carcinoma." J Natl Cancer Inst **51**(5): 1409-1416.

Sternberg, C. N., A. Yagoda, H. I. Scher, R. C. Watson, N. Geller, H. W. Herr, M. J. Morse, P. C. Sogani, E. D. Vaughan, N. Bander and et al. (1989). "Methotrexate, vinblastine, doxorubicin, and cisplatin for advanced transitional cell carcinoma of the urothelium. Efficacy and patterns of response and relapse." Cancer **64**(12): 2448-2458.

Stordal, B. and M. Davey (2007). "Understanding cisplatin resistance using cellular models." IUBMB Life **59**(11): 696-699.

Takahashi, T., N. Boku, H. Murakami, T. Naito, A. Tsuya, Y. Nakamura, A. Ono, N. Machida, K. Yamazaki, J. Watanabe, A. Ruiz-Garcia, K. Imai, E. Ohki and N. Yamamoto (2012). "Phase I and pharmacokinetic study of dacomitinib (PF-00299804), an oral irreversible, small molecule inhibitor of human epidermal growth factor receptor-1, -2, and -4 tyrosine kinases, in Japanese patients with advanced solid tumors." Invest New Drugs **30**(6): 2352-2363.

Tiseo, M., R. Andreoli, F. Gelsomino, P. Mozzoni, C. Azzoni, M. Bartolotti, B. Bortesi, M. Goldoni, E. M. Silini, G. De Palma, A. Mutti and A. Ardizzoni (2014). "Correlation between erlotinib pharmacokinetics, cutaneous toxicity and clinical outcomes in patients with advanced non-small cell lung cancer (NSCLC)." Lung Cancer **83**(2): 265-271.

Vaught, D. B., J. C. Stanford, C. Young, D. J. Hicks, F. Wheeler, C. Rinehart, V. Sanchez, J. Koland, W. J. Muller, C. L. Arteaga and R. S. Cook (2012). "HER3 is required for HER2-induced preneoplastic changes to the breast epithelium and tumor formation." Cancer Res **72**(10): 2672-2682.

Vishnu, P., J. Mathew and W. W. Tan (2011). "Current therapeutic strategies for invasive and metastatic bladder cancer." Onco Targets Ther **4**: 97-113.

Wood, D. P., Jr., A. E. Anderson, R. Fair and R. S. Chaganti (1992). "Ras oncogene point mutations in bladder cancer resistant to cisplatin." Urol Res **20**(4): 313-316.

Wu, H. C., J. T. Hsieh, M. E. Gleave, N. M. Brown, S. Pathak and L. W. Chung (1994). "Derivation of androgen-independnet human LNCaP prostatic cancer cell sublines: role of bone stromal cells." Int J Cancer **57**(3): 406-412.

Wu, W. S. (2006). "The signaling mechanism of ROS in tumor progression." Cancer Metastasis Rev **25**(4): 695-705.

Wulfing, C., J. P. Machiels, D. J. Richel, M. O. Grimm, U. Treiber, M. R. De Groot, P. Beuzeboc, R. Parikh, F. Petavy and I. A. El-Hariry (2009). "A single-arm, multicenter, open-label phase 2 study of lapatinib as the second-line treatment of patients with locally advanced or metastatic transitional cell carcinoma." Cancer **115**(13): 2881-2890.

Yarden, Y. and M. X. Sliwkowski (2001). "Untangling the ErbB signalling network." Nat Rev Mol Cell Biol **2**(2): 127-137.

Yoo, J. Y., X. W. Wang, A. K. Rishi, T. Lessor, X. M. Xia, T. A. Gustafson and A. W. Hamburger (2000). "Interaction of the PA2G4 (EBP1) protein with ErbB-3 and regulation of this binding by heregulin." Br J Cancer **82**(3): 683-690.

Zachos, I., P. A. Konstantinopoulos, V. Tzortzis, S. Gravas, A. Karatzas, M. V. Karamouzis, M. Melekos and A. G. Papavassiliou (2010). "Systemic therapy of metastatic bladder cancer in the molecular era: current status and future promise." Expert Opin Investig Drugs **19**(7): 875-887.

Zhang, J., H. Tang, Y. Zhang, R. Deng, L. Shao, Y. Liu, F. Li, X. Wang and L. Zhou (2014). "Identification of suitable reference genes for quantitative RT-PCR during 3T3-L1 adipocyte differentiation." Int J Mol Med **33**(5): 1209-1218.